

<https://doi.org/10.1038/s41612-025-01280-w>

# Three generations of NARClIM: future projections of mean and extreme climate over the CORDEX Australasia domain

Check for updates

Fei Ji<sup>1</sup> ✉, Moutassem El Rafei<sup>1,2</sup>, Giovanni Di Virgilio<sup>1,2</sup>, Jason P. Evans<sup>2,3</sup>, Jatin Kala<sup>4</sup>, Stephen White<sup>1</sup>, Julia Andrys<sup>4</sup>, Dipayan Choudhury<sup>1</sup>, Eugene Tam<sup>1</sup>, Yue Li<sup>1</sup>, Rishav Goyal<sup>1</sup>, Carlos Vieira Rocha<sup>1</sup> & Matthew L. Riley<sup>1</sup>

Regional climate simulations provide essential high-resolution information for climate services. This study evaluates future changes in mean climate and 10 extremes using three generations of the NARClIM (NSW and Australian Regional Climate Modelling) project, which downscale CMIP3, CMIP5, and CMIP6 models. Projections show statistically significant increases in maximum and minimum temperatures across all NARClIM generations, with consistent spatial patterns. The magnitude of warming is primarily influenced by driving GCMs and emissions scenarios. In contrast, precipitation projections exhibit greater variability between generations, reflecting model and scenario differences and underscoring the challenge of projecting future precipitation. Extreme heat indices are projected to increase across Australia, with consistent spatial patterns and stronger changes under higher emissions, indicating more frequent and severe extreme heat events. Precipitation extremes display more variability across regions, model generations, and scenarios, although certain trends are robust. The intensity of very extreme rainfall (above the 99th percentile) is projected to increase, as is the maximum length of dry spells. Conversely, the maximum length of wet spells and the number of heavy rain days are expected to decrease. NARClIM2.0 specifically suggests shorter wet periods and fewer heavy rain days, but more intense extreme rainfall. These findings demonstrate the relative robustness of temperature and its extremes compared to precipitation and emphasize the value of broader GCM ensembles in future downscaling efforts to improve confidence in regional projections.

Regional climate projections are essential for translating the global-scale impacts of climate change into practical, regionalised strategies that address region-specific challenges and help build climate resilience<sup>1</sup>. Regional climate simulations have emerged as a critical resource for climate services at regional scales, providing more detailed, regional-scale projections<sup>2–4</sup>.

Several prominent downscaling programs have been developed globally, each making substantial contributions to regional climate projections. Initiatives such as PRUDENCE<sup>5</sup>, ENSEMBLES<sup>6</sup>, RMIP<sup>7</sup>, NARCCAP<sup>8</sup>, and CLARIS-LPB<sup>9</sup> have collectively advanced our understanding of regional climate variability and projected future changes. These programs employ diverse downscaling techniques to refine the coarse outputs of global climate models (GCMs), resulting in higher-resolution regional climate projections.

The CORDEX (COordinated Regional Downscaling EXperiment) initiative is a global effort to coordinate regional downscaling activities, ensuring consistency and comparability among regional climate projections across 14 designated regions worldwide<sup>10</sup>. By offering standardized datasets and methodologies, CORDEX supports comprehensive assessments of regional climate change and its impacts, aiding stakeholders in formulating robust climate adaptation strategies.

In Australasia, multiple modelling groups have dynamically downscaled CMIP6 (Coupled Model Intercomparison Project phase 6) GCMs as part of their contributions to CORDEX Australasia<sup>11–14</sup>. Among these, the NARClIM (NSW and Australian Regional Climate Modelling) project represents a significant regional dynamical downscaling initiative (Fig. 1)

<sup>1</sup> Climate & Atmospheric Science, NSW Department of Climate Change, Energy, the Environment and Water, Sydney, NSW, Australia. <sup>2</sup> Climate Change Research Centre, University of New South Wales, Sydney, NSW, Australia. <sup>3</sup> Australian Research Council Centre of Excellence for 21st Century Weather, University of New South Wales, Sydney, NSW, Australia. <sup>4</sup> Environmental and Conservation Sciences, and Centre for Climate Impacted Terrestrial Ecosystems, Harry Butler Institute, Murdoch University, Murdoch, WA, Australia. ✉ e-mail: [fei.ji@dcceew.nsw.gov.au](mailto:fei.ji@dcceew.nsw.gov.au)

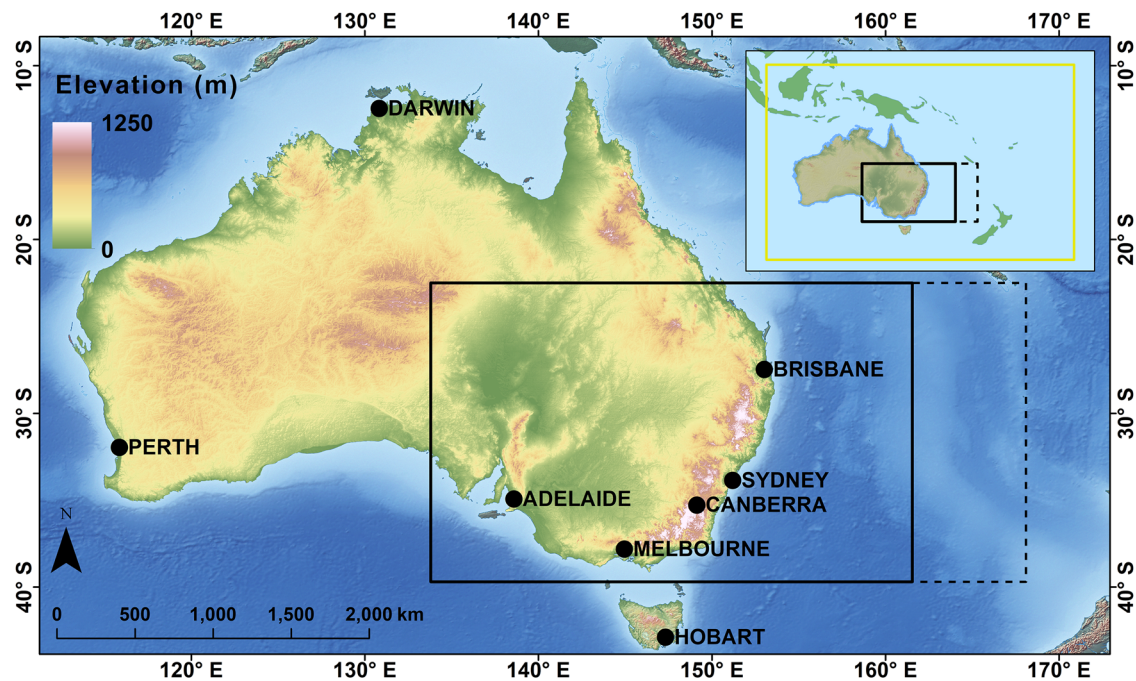


**Fig. 1 | Topographic variation across Australia and major cities.** Inset: The CORDEX-Australasia domain. All NARClIM RCMs are run using two nested domains via one-way nesting with an outer domain over CORDEX Australasia and an inner domain over south-eastern Australia (black rectangle in both main panel

and inset). Black dashed rectangle is the inner domain extent for NARClIM1.0 and 1.5; rectangle with solid black lines is the inner domain extent for NARClIM2.0. Solid dots represent locations of eight state capital cities. (Adopted from Di Virgilio et al.<sup>14</sup>).

and constitutes one of the contributions to CORDEX Australasia. Like other programs, NARClIM generates finer-scale future climate projections tailored to regional needs. To date, NARClIM has completed three major phases: the first generation (N1.0) delivered in 2014<sup>15</sup>, the second generation (N1.5) delivered in 2020<sup>16</sup>, and the third generation (N2.0) delivered in 2024<sup>14</sup>. These phases have dynamically downscaled GCM outputs from the Coupled Model Intercomparison Project phases 3, 5, and 6 (CMIP3, CMIP5, and CMIP6), respectively. Each successive NARClIM phase has progressively enhanced the resolution and accuracy of regional climate simulations<sup>17</sup>, thereby improving their utility for climate impact assessments and future planning.

Numerous studies have used NARClIM simulations to project future changes in both mean climate and climate extremes. These simulations provide critical insights into regional climate impacts, which are essential for decision-making in climate adaptation and risk management. Olson et al.<sup>18</sup> employed N1.0 outputs to project future changes in rainfall and temperature, assessing the degree of model agreement on climate change signals. Their work provided important benchmarks for understanding regional shifts in rainfall patterns and temperature trends. Similarly, Evans et al.<sup>19</sup> applied N1.0 simulations to assess projections of extreme rainfall, contributing valuable information about future flood risks and storm intensity. Herold et al.<sup>20</sup> focused on the future frequency of climate extremes, utilizing N1.0 simulations to project how events like heatwaves and extreme rainfall might become more frequent. Their findings reinforced the importance of addressing the increasing occurrence of extreme events under climate change. Evans et al.<sup>21</sup> explored the resilience of Australian wind energy systems to projected future climate scenarios by using N1.0 simulations, demonstrating the potential impacts of changing wind patterns on energy infrastructure and capacity.

Di Luca et al.<sup>22</sup> assessed future changes in snowpack over the Australian Alps with N1.0 simulations. Their analysis indicated a potential decline in snowpack, with implications for water resources, ecosystems, and tourism in the region. Ji et al.<sup>23,24</sup> investigated changes in near-surface temperature inversions and vertical temperature profiles using N1.0 and 1.5 simulations. These studies highlighted critical shifts in temperature stratification, which

can affect atmospheric stability and weather patterns. Di Virgilio et al.<sup>25,26</sup> focused on extreme wildfire risk, using N1.0 simulations to examine potential changes in wildfire behaviour under future climate conditions. The results indicated increased risk of extreme wildfires, providing valuable information for fire management and planning. Nishant et al.<sup>16</sup> compared projections of precipitation and temperature between N1.0 and 1.5, highlighting both similarities and differences in the two model generations' results.

Further comparisons were made by Ji et al.<sup>27,28</sup>, who examined projections of selected precipitation and temperature extremes between N1.0 and 1.5 and identified rapid warming trends in the Australian Alps—a key region for biodiversity and water supply. Evans et al.<sup>29</sup> broadened the comparison by analysing CORDEX-Australasia ensembles for future climate projections, incorporating N1.5 simulations. In addition to these academic studies, N1.0 and N1.5 simulations have been included in national-level climate projection services such as Climate Change in Australia (<https://www.climatechangeinaustralia.gov.au/en/>) and hydrological projections<sup>30</sup>. These applications demonstrate the broad utility of NARClIM outputs in supporting climate adaptation strategies and risk assessment across various sectors in Australia.

With the release of N2.0, it is essential to conduct a comprehensive comparison across the three generations of NARClIM to thoroughly assess differences and similarities in projected temperature and precipitation. Such a comparison will help identify changes in regional climate projections, and the consistency of trends across generations. Understanding these details is critical for improving confidence in future climate projections and refining adaptation strategies. Additionally, the comparison will provide valuable insights into how evolving models influence the interpretation of climate impacts, supporting better decision-making in climate-sensitive sectors.

The aim of this study is to systematically compare future climate projections from these three generations of NARClIM. Specifically, we examine similarities and differences in projected changes to mean climate and extremes, assess how updates in driving GCMs, emission scenarios, and model resolution contribute to these differences, and evaluate the robustness of projections across generations. Through this comparison, we provide a

clearer understanding of the evolution of regional climate projections for Australia, and their implications for climate risk assessment and adaptation planning.

## Results

### Future projections of mean climate

In this section, we compare future projections of maximum and minimum temperatures, and precipitation across the three NARCLiM generations. We evaluate the similarities and differences in future projections among these generations. The ensemble mean of future projections is presented in the main text, while projections for individual ensemble members are provided in the supplementary material.

We first assess annual mean maximum temperature. Historical simulations from all three NARCLiM generations show a consistent spatial pattern of maximum temperature across Australia, reflecting the models' reliability in reproducing observed distributions (Supplementary Fig. S1a, j, p). Among them, N1.0 simulates slightly cooler annual mean maximum temperatures than N1.5, and substantially cooler than N2.0, indicating a progressive warming trend in newer model generations.

N2.0 projects significant increases in maximum temperatures across Australia, with the magnitude of warming varying by location and emission scenario (Fig. 2a–o). Central Australia is projected to warm more than northern and southern regions, including Tasmania, with the largest increases occurring along the inland New South Wales and Southwest Queensland during summer (Fig. 2b, g, l). Under the high-emission scenario (SSP3–7.0), widespread and pronounced warming is projected (Fig. 2a), with domain averaged annual increase of 2.76 °C, while SSP1–2.6 projects a relatively cooler future than other emissions (Fig. 2k), with domain averaged annual increase of 1.39 °C, and SSP2–4.5 shows intermediate warming (Fig. 2f). Seasonal variations align with the annual warming pattern, but the magnitude differs: winter (JJA) exhibits the smallest increases, while the season of greatest warming depends on the scenario—spring (SON) under SSP3–7.0, summer (DJF) under SSP2–4.5 and SSP1–2.6 (Fig. 2; Supplementary Figs. S2–S5, S16–S20).

N1.5 projects an even hotter future under RCP8.5, with a domain-averaged annual increase of 3.29 °C—higher than both N1.0 and N2.0 (Fig. 2p; Supplementary Fig. S11). While the spatial warming pattern is consistent with other generations, the intensity is greater. Under RCP4.5, the domain-averaged increase is 2.06 °C (Fig. 2u; Supplementary Fig. S1o), close in magnitude to SSP2–4.5 projections from N2.0. N1.5 shows similar seasonal variations to N2.0, with smaller increases in winter and greater increases in spring and summer, demonstrating strong sensitivity to emission scenarios.

N1.0 also projects significant warming, with a domain-averaged annual increase of ~2.25 °C—between SSP2–4.5 and SSP3–7.0 projections. The spatial warming pattern differs slightly, with the largest increases concentrated in western central Australia (Fig. 2z; Supplementary Fig. S1r). Seasonal variation is consistent with N2.0 and N1.5, with the least warming in winter and the most in spring and summer. Future increases in maximum temperatures for eight state capital cities are listed in Supplementary Table S3.

Historical simulations across all three NARCLiM generations consistently reproduce the spatial distribution of minimum temperatures (Supplementary Fig. S6a, S6j, S6p), indicating consistent model performance. N2.0 projects significant increases in minimum temperatures across Australia, with largest increase along the inland New South Wales and Southwest Queensland during summer. For high-emission scenarios, N2.0's warming lies between N1.0 and N1.5, with domain average increase of 2.83 °C (Fig. 3a; Supplementary Figs. S6c, S21–S25), reflecting a moderate outcome. Minimum temperature projections under SSP1–2.6 are significantly cooler than those under SSP3–7.0, with domain average increase of 1.33 °C, while SSP2–4.5 lies in between (Fig. 3a, f, k; Supplementary Fig. S6c, f, i), underscoring the influence of emissions trajectories.

N1.5 projects greater warming than N1.0 under RCP8.5, with a domain-averaged increase of 2.85 °C (Fig. 3p), and a much smaller increase under RCP4.5 (Fig. 3u). While the spatial pattern resembles N1.0, the

magnitude is stronger under high emissions, highlighting an intensified warming trend in the mid-generation model.

N1.0 shows significant increasing minimum temperatures across Australia, generally mirroring the maximum temperature trends (Figs. 2z, 3z). Larger increases occur in central west and central east Australia, while coastal and southern areas, including Tasmania, experience smaller increases (Supplementary Fig. S6r). The domain-averaged warming is ~2.28 °C.

Seasonal variations in minimum temperature projections are evident across all models and scenarios, with winter showing the smallest increases and other seasons experiencing greater warming (Fig. 3; Supplementary Figs. S7–S10). Future increases in annual and seasonal minimum temperatures for eight state capital cities are listed in Supplementary Table S4.

While all three NARCLiM generations simulate a similar spatial pattern of annual precipitation for the historical period, their magnitudes differ. N1.0 produces the highest Australia-averaged precipitation, followed by N1.5, with N2.0 showing the lowest values (Supplementary Fig. S11a, j, p), indicating a decreasing trend across generations.

N2.0 projects a complex pattern of precipitation changes across emission scenarios. Under SSP3–7.0, modest increases are projected for Northern Australia, minimal change for central regions, and decreases across southwest and eastern Australia, including Tasmania (Fig. 4a; Supplementary Figs. S26–S30). The largest increase is projected in Northern Australia in summer and the largest decrease in Southwest Western Australia in winter. SSP2–4.5 exhibits similar spatial patterns but with lower magnitude changes (Fig. 4f). The SSP1–2.6 projection differs more substantially, especially in Northern Australia, emphasizing the strong sensitivity of precipitation outcomes to emissions (Fig. 4k). These changes in precipitation are mostly statistically insignificant except for large decrease in Southwest Western Australia.

N1.5 presents a more localized and variable pattern than either N1.0 or N2.0. Under both RCP8.5 and RCP4.5, N1.5 projected increases in precipitation over central Western Australia and western Tasmania but substantial decreases elsewhere (Fig. 4p, u). These changes are more pronounced under RCP8.5, showing stronger contrasts between wet and dry regions (Supplementary Fig. S11i, o), and reflecting N1.5's high variability and regional sensitivity. The largest increase is projected in Central Western Australia in winter but the largest decrease in Southeastern Australia in Spring.

N1.0 shows clearer large-scale wetting and drying patterns. Drying is projected in southwest Australia, Victoria, and Tasmania, while northern and central Australia are projected to become wetter (Fig. 4z; Supplementary Fig. S11r). While more spatially coherent, N1.0 lacks the localized contrast captured by N1.5 and N2.0. The largest increase is projected in central Northern Australia in Summer and the largest decrease in southwest Western Australia, Victoria and Tasmania in Spring.

In contrast to temperature projections, seasonal variation in precipitation is inconsistent across model generations, emission scenarios, and regions (Fig. 4; Supplementary Figs S12–S15), making projections more uncertain. Future changes in annual and seasonal precipitation for eight state capital cities are listed in Supplementary Table S5.

In summary, projections across all NARCLiM generations consistently show robust and statistically significant warming trends in both maximum and minimum temperatures. The magnitude of change depends on the model generation and emission scenario, with N2.0 and N1.5 often projecting stronger warming under high emissions. Seasonal variations are well defined, with winter generally showing the least warming. Precipitation projections are more variable and uncertain. Differences across generations, emission scenarios, and geographic regions highlight the complexity of simulating precipitation responses. While N1.0 provides more coherent wetting/drying patterns, N1.5 and N2.0 capture finer-scale variability. These uncertainties underline the need for care to be taken when interpreting or applying precipitation projections in climate impact assessments.

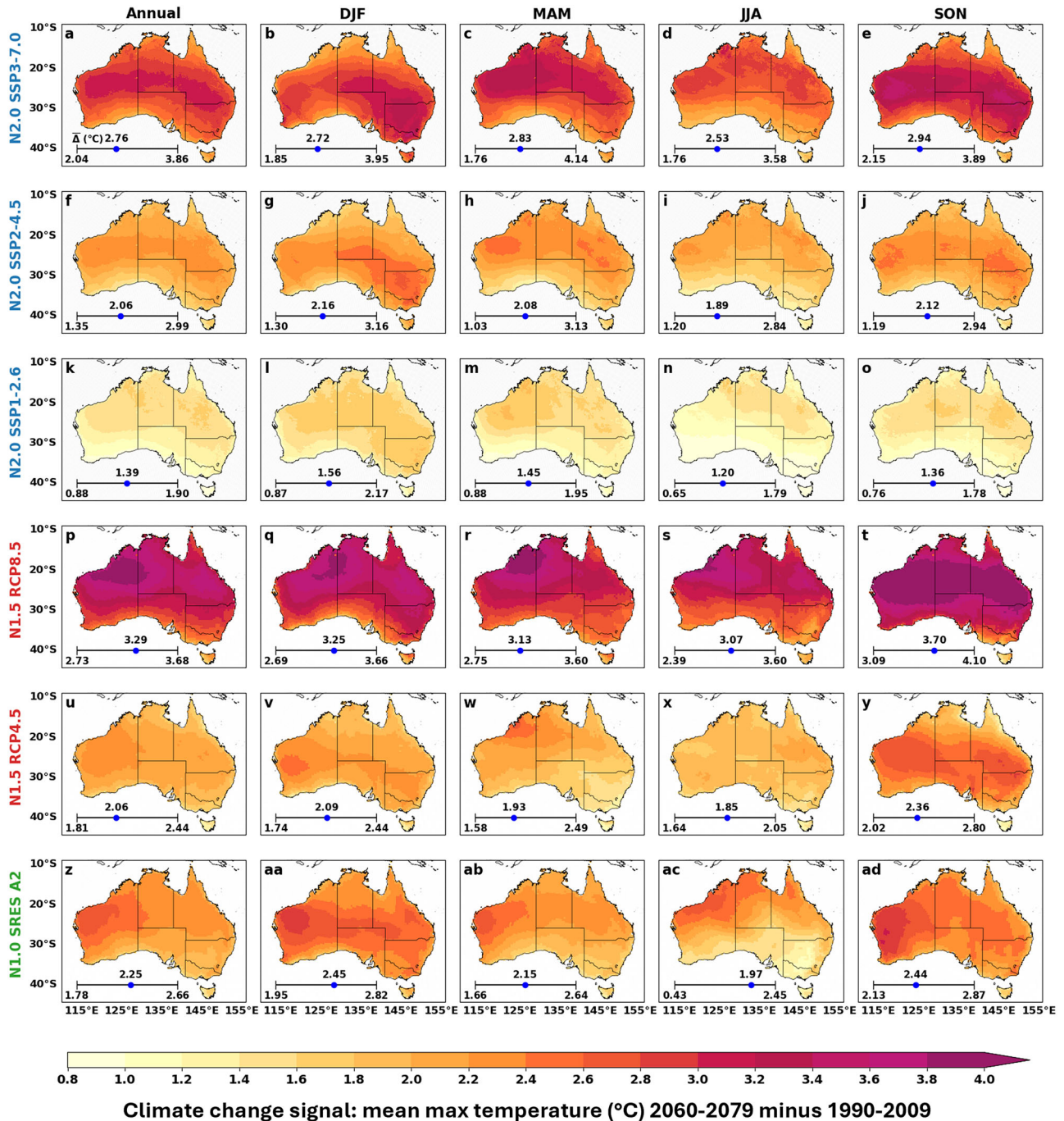


**Fig. 2 | Ensemble mean changes in annual and seasonal maximum temperature for three NARClIM generations. a–e, f–j, and k–o illustrate the annual and seasonal changes in maximum temperature for NARClIM2.0 under SSP3-7.0, SSP2-4.5, and**

**SSP1-2.6, respectively. p–t and u–y show the corresponding changes for NARClIM1.5 under RCP8.5 and RCP4.5, respectively. z–ad present the annual and seasonal changes in maximum temperature for NARClIM1.0 under SRES A2.**

**Similarities and differences in future projections of mean climate**

Clear similarities exist across the three generations of NARClIM, with consistent spatial patterns of temperature change. Maximum and minimum temperatures are projected to significantly increase across Australia, with greater warming in central and northern regions compared to the south, including Tasmania. Seasonal variations show that temperature increases will be more pronounced in summer, spring and autumn than in winter. Importantly, N2.0 shows increases in summertime maximum and minimum temperatures are strongest over economically important areas of southeastern Australia (Figs. 2b, g, l, 3b, g, l). Additionally, all model generations generally project stronger warming and precipitation changes under high-emission scenarios compared to low-emission ones, while

historical simulations capture similar spatial precipitation patterns, each generation exhibits distinct regional changes in response to different emission scenarios.

Nevertheless, substantial differences exist between NARClIM generations. Maximum and minimum temperatures increase across all models, with N1.5 projecting the highest warming under RCP8.5, while N2.0 sits between N1.0 and N1.5 for high emissions. Precipitation responses also vary: N1.0 projects wetter conditions in central and northern Australia but drier conditions in the southwest; N1.5 shows increased rainfall in central-western areas but drier conditions elsewhere. The increase came from the CanESM2 driven simulations only<sup>29</sup>. N2.0 indicates slight increases in northern Australia but significant drying in the east and southwest. Overall,

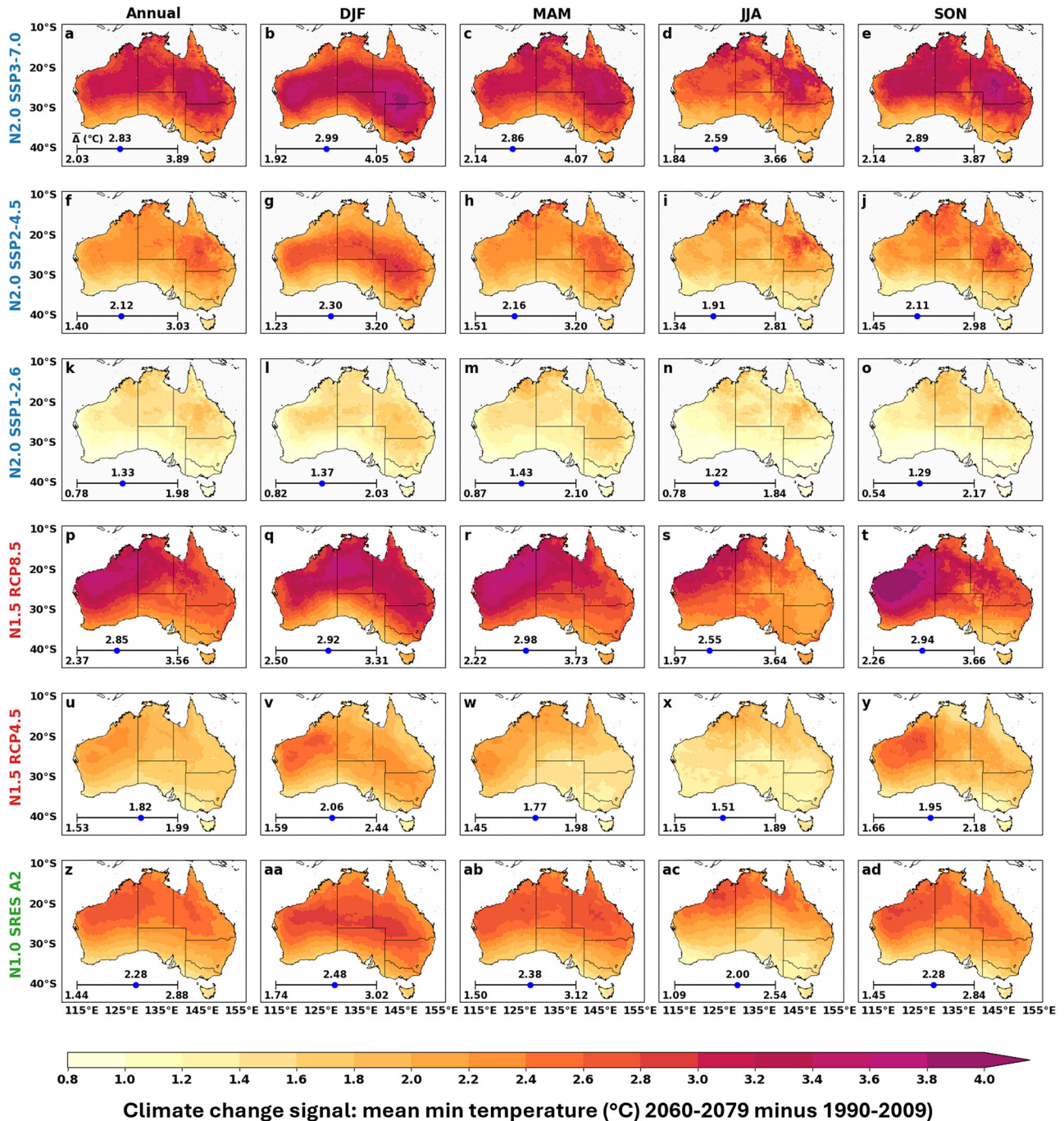


**Fig. 3 | Ensemble mean changes in annual and seasonal minimum temperature for three NARClM generations, with significance stippling as per Fig. 2. a–e, f–j, and k–o illustrate the annual and seasonal changes in minimum temperature for NARClM2.0 under SSP3-7.0, SSP2-4.5, and SSP1-2.6, respectively.**

p–t and u–y show the corresponding changes for NARClM1.5 under RCP8.5 and RCP4.5, respectively. z–ad present the annual and seasonal changes in minimum temperature for NARClM1.0 under SRES A2.

newer generations (N1.5 and N2.0) project warmer and drier conditions than N1.0, indicating a shift toward more intense warming and drying trends. Furthermore, N2.0 adopts SSP-based scenarios and shows greater sensitivity to emissions, with SSP1–2.6 producing substantially lower warming than high-emission scenarios, reinforcing the importance of emission reductions.

Overall, while all generations consistently project warming trends over Australia, a key difference for temperature projections is in the magnitude of warming. In contrast, precipitation projections show substantially different spatial patterns, albeit most of these changes are often statistically

insignificant. These differences highlight the impact of model updates and emission scenario variations on future climate projections.

The temperature projections across the three generations of NARClM show strong consistency with their respective driving GCMs (Figs. 2, 3, 5). In contrast, precipitation projections display only general alignment with the driving GCMs (Figs. 4, 6). On average, the GCMs used in N1.5 are hotter than those in N2.0 and significantly hotter than those in N1.0 under high-emission scenarios (Fig. 7). This indicates that regional temperature outcomes in NARClM closely follow the patterns set by their driving GCMs. Additionally, emission scenarios play a substantial role, with higher

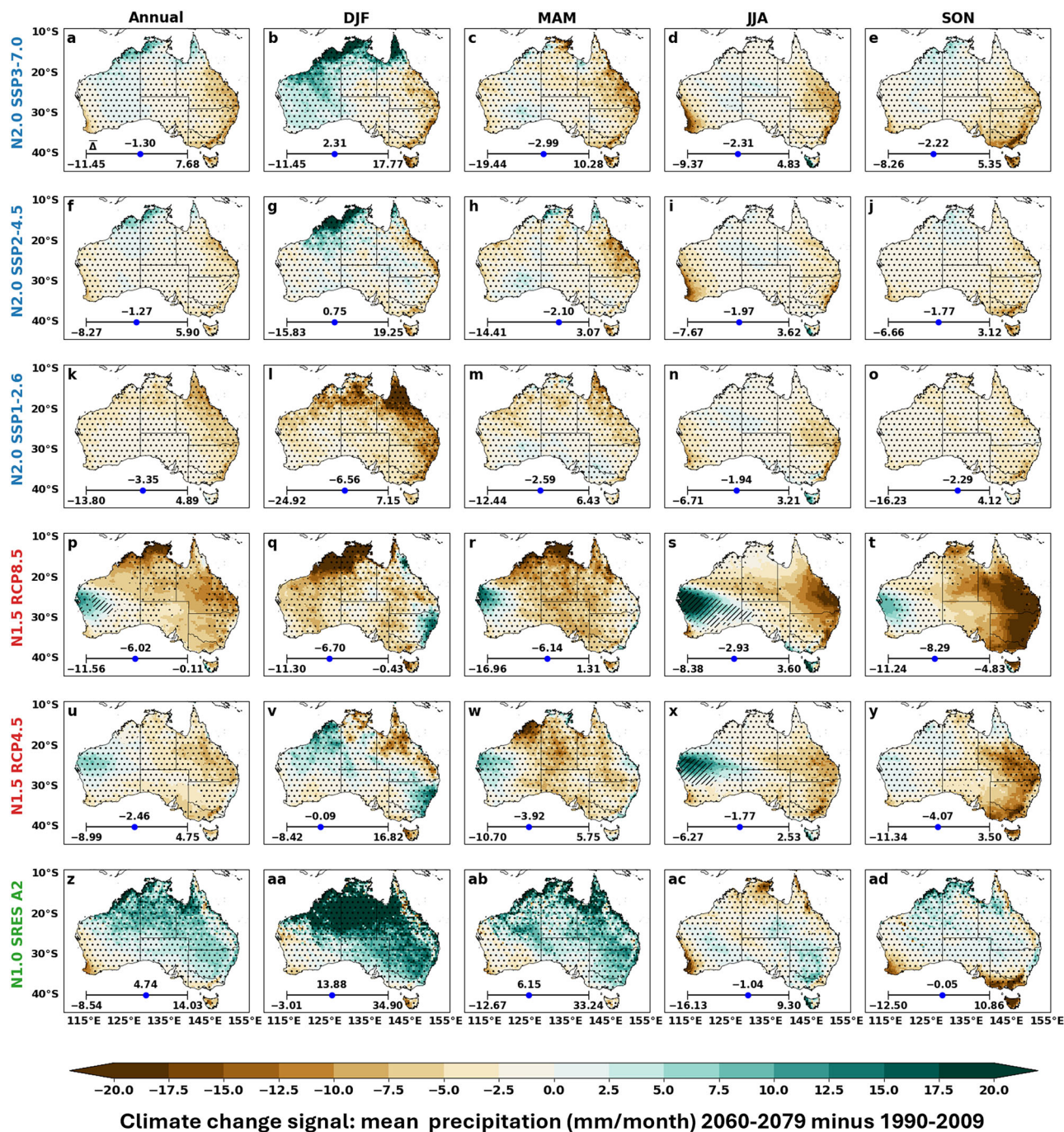


**Fig. 4 | Ensemble mean changes in annual and seasonal precipitation for three NARClm generations, with significance stippling as per Fig. 2. a–e, f–j, and k–o illustrate the annual and seasonal changes in precipitation for NARClm2.0 under SSP3-7.0, SSP2-4.5, and SSP1-2.6, respectively. p–t and u–y show the**

corresponding changes for NARClm1.5 under RCP8.5 and RCP4.5, respectively. z–ad present the annual and seasonal changes in precipitation for NARClm1.0 under SRES A2.

emissions leading to significantly hotter projections, consistent with findings from previous studies<sup>31–33</sup>. This relationship highlights the critical role of emission pathways in determining future climate conditions.

However, precipitation projections show substantial differences between NARClm generations. In N1.0, two of the driving GCMs are classified as wet models, while the other two are slightly dry (Fig. 7). This combination results in a wet ensemble mean projection for southeast Australia (Fig. 4z). The wet projections for southeast and northern Australia in N1.0 are likely inherited from these driving GCMs, as the GCMs significantly influence regional climate simulations. Compared to N1.0, three GCMs in N1.5 are hotter, and two of them are very dry (Fig. 7). The dry

future projections in N1.5 are primarily inherited from these driving GCMs, emphasizing hotter and drier conditions. In N2.0, three out of five GCMs used are relatively dry (Fig. 7). We also note that most CMIP6 GCMs projected reductions in mean precipitation over southeast Australia (Fig. 7). Consequently, the relatively dry projections in N2.0 are likely derived from these driving GCMs, shaping the overall climate outcomes in the model ensemble.

Results from N1.0 and N2.0 are sometimes similar (e.g. patterns and magnitude of future changes in temperatures and their extremes) but differ substantially from N1.5, reflecting design choices. Future projections across all NARClm generations are strongly shaped by the driving GCMs. For

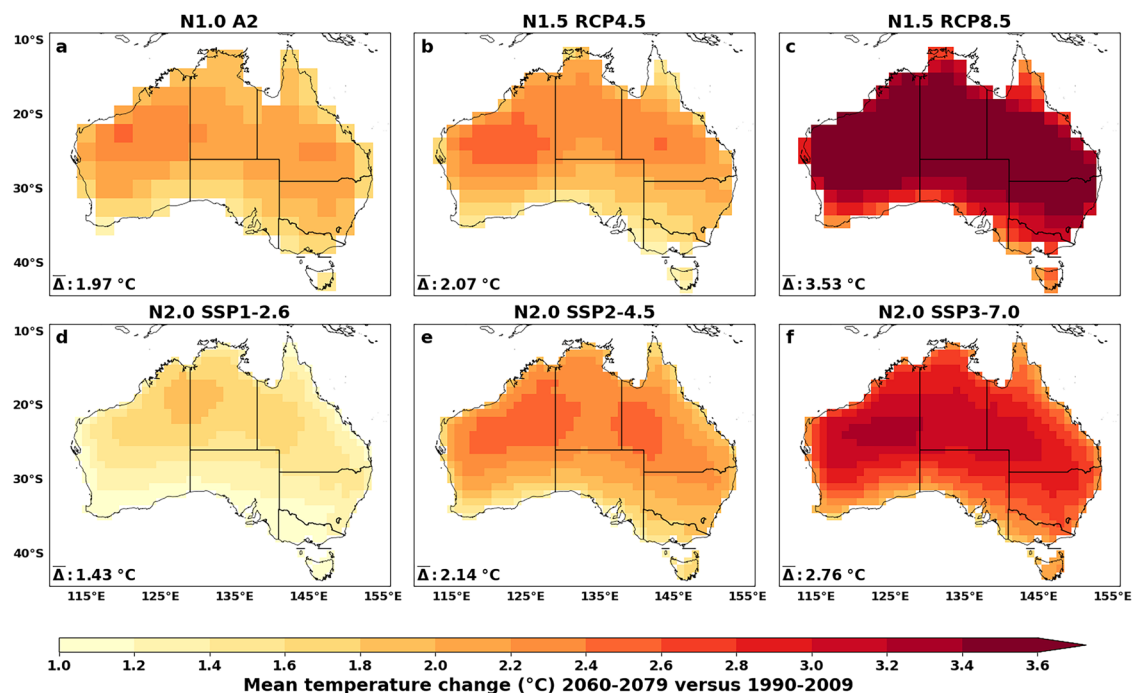


**Fig. 5 | Ensemble mean changes in GCM simulated mean temperature for three NARCLiM generations.** **a** shows the ensemble mean of future changes in GCM-simulated mean temperature for NARCLiM1.0 under SRES A2. **b** and **c** show the ensemble mean of future changes in GCM-simulated mean temperature for NARCLiM1.5 under RCP4.5 and RCP8.5, respectively. **d–f** show the ensemble mean of future changes in GCM-simulated mean temperature for NARCLiM2.0 under SSP1-2.6, SSP2-4.5, and SSP3-7.0, respectively.

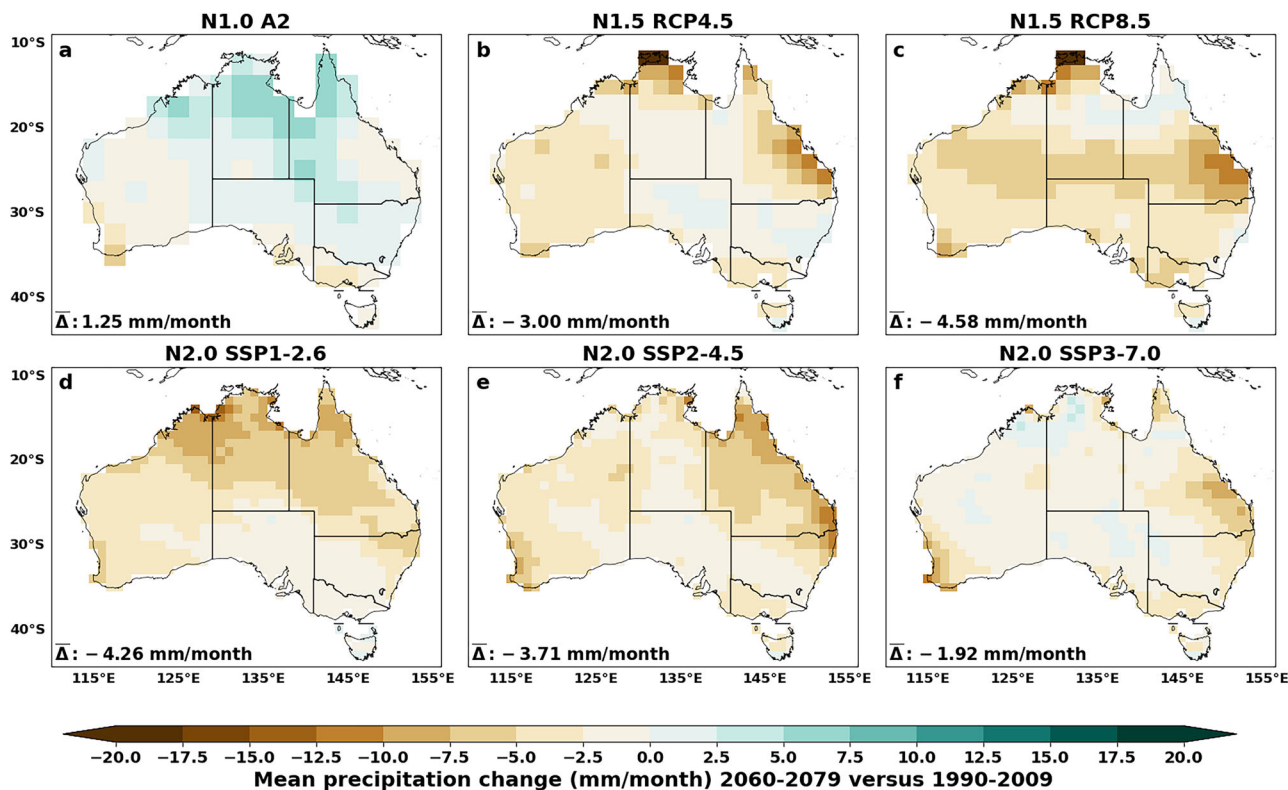
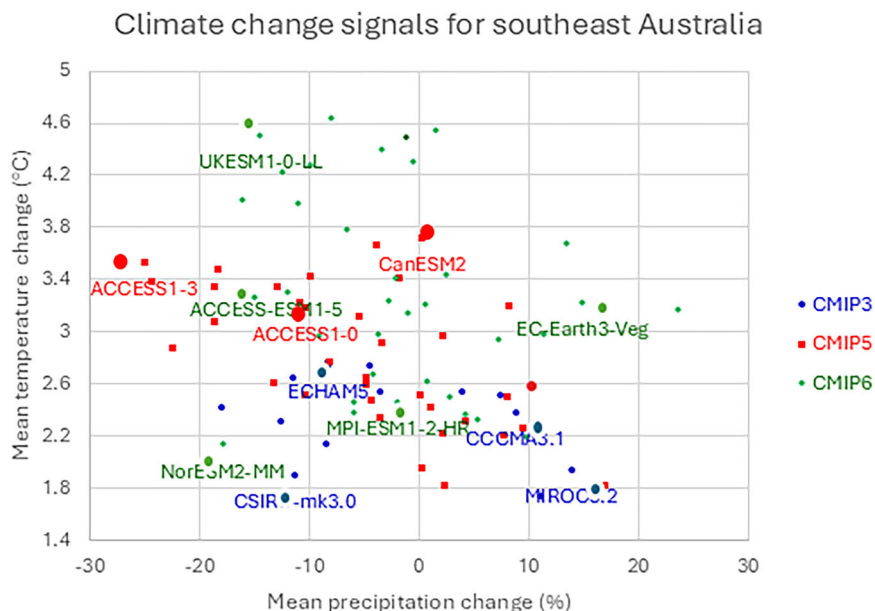


**Fig. 6 | Ensemble mean changes in GCM simulated precipitation for three NARCLiM generations.** **a** shows the ensemble mean of future changes in GCM-simulated precipitation for NARCLiM1.0 under SRES A2. **b** and **c** show the ensemble mean of future changes in GCM-simulated precipitation for NARCLiM1.5 under RCP4.5 and RCP8.5, respectively. **d–f** show the ensemble mean of future changes in GCM-simulated precipitation for NARCLiM2.0 under SSP1-2.6, SSP2-4.5, and SSP3-7.0, respectively.

**Fig. 7 | Scatter plot of future change (differences between 2060–2079 and 1990–2009) in precipitation and temperature over the land part of the NARcliM domain (Fig. 1) for 36 CMIP6 GCMs (green) for SSP3–7.0, 34 CMIP5 GCMs (blue) for RCP8.5 and 14 CMIP3 GCMs (red) for SRES A2 that passed the performance test. Larger dots represent the five GCMs selected for N2.0 (green), the three GCMs selected for N1.5 (red) and the four GCMs selected for N1.0 (blue).**



N1.0 and N2.0, GCMs were selected using four criteria: good performance in simulating observed climate, independence of model biases, representation of the full range of projected changes for southeast Australia, and data availability<sup>14,15</sup>. These ensembles reproduce historical climate more reliably, are largely independent, and together span the full range of changes in CMIP3 and CMIP6 (Fig. 7). In contrast, N1.5 was designed to downscale CMIP5 GCMs, complementing N1.0 by sampling outcomes under-represented in CMIP3<sup>16</sup>. Its three GCMs are all hot, with two also dry, highlighting sharper contrasts compared with the more balanced spread of N1.0 and N2.0. Scenario design also differed across NARcliM generations. In terms of emissions narratives, SRES A2 used in N1.0 is broadly more similar to SSP3–7.0 in N2.0 than to RCP8.5 in N1.5 (Supplementary Tables S1, S2).

In summary, the precipitation and temperature projections in NARcliM are heavily influenced by the characteristics of their driving GCMs and the emission scenarios used. Wet or dry tendencies in the driving GCMs are inherited by the regional models, shaping Australia’s overall climate projections.

**Future projections of climate extremes**

In this section, we compare future projections of 10 selected temperature and precipitation extremes between the three generations of NARcliM. We assess the similarity and differences in future projections between generations and between scenarios.

First, we assess future projections of temperature-related extremes across the three NARcliM generations. Five selected temperature-related indices—TXx, TNn, DTR, TXge35, and WSDI—are evaluated and compared below.

TXx (Annual maximum value of daily maximum temperature): N2.0 shows a consistent spatial pattern of significant increases in TXx as maximum temperature across all three SSP scenarios (Figs. 2, 8). Under SSP3–7.0, N2.0 projects the largest domain-averaged TXx increase (2.84 °C), followed by SSP2–4.5 (2.15 °C), while SSP1–2.6 shows the smallest rise (1.46 °C) (Fig. 8a, f, k). The largest increase is observed in southeast Australia and the least in Northern Australia. Notably, the increase in TXx exceeds that of the mean maximum temperature (Fig. 2a, f, k), indicating an intensification of extreme heat events in futures.

N1.5 exhibits a similar spatial pattern of TXx increases under both RCP8.5 and RCP4.5 (Fig. 8p, u), though the magnitude differs significantly between scenarios. Under RCP8.5, N1.5 projects a large domain-averaged TXx increase of 3.37 °C, which exceeds the corresponding increase in mean

maximum temperature (3.29 °C) and indicates more intense extreme heat (Supplementary Fig. S311). The largest increase is observed in central Western Australia. For RCP4.5, the TXx increase is notably smaller, closely aligning with the rise in mean maximum temperature (Figs. 2u, 8u).

N1.0 also projects a significant increase in TXx, particularly over inland Western Australia and along the Great Dividing Range (Fig. 8z), consistent with the pattern of mean annual maximum temperature increases (Fig. 3z). The domain-averaged TXx rise (2.57 °C) is higher than the increase in mean maximum temperature (2.25 °C), indicating a future intensification of extreme heat events.

TNn (Annual Minimum Value of Daily Minimum Temperature): N2.0 projects a significant increase in TNn, particularly along the northern Australian coasts and northeastern Australia, with the strongest increases under higher emission scenarios, with domain average increase of 2.41 °C under SSP3–7.0. Across all scenarios and NARcliM generations, TNn increases are generally smaller than those in mean minimum temperature (Fig. 3), and notably smaller than TXx increases—especially under high-emission scenarios—highlighting a stronger intensification of extreme heat events relative to cold extremes in future climates.

N1.5 projects a similar spatial pattern of TNn increases to N1.0 & 2.0 under both RCP8.5 and RCP4.5 (Fig. 8q, v). Under RCP8.5, the domain-averaged TNn increase reaches 2.27 °C, which is substantially higher than in N1.0. Under RCP4.5, the TNn increase is slightly smaller than that of N1.0. N1.0 also shows significant increases in TNn, with the largest changes occurring in Northern Australia (Fig. 8aa, Supplementary Fig. S32s). The domain-averaged TNn rise is ~1.68 °C.

Compared to TXx, future increases in TNn are generally larger in Northern Australia but smaller elsewhere (Supplementary Fig. S41), which aligns well with recent findings by Chapman et al.<sup>11</sup>. This asymmetry reflects strong land–atmosphere feedback. In Northern Australia, the larger increase in TNn than TXx is due to strong moisture and cloud feedback that limit daytime heating but enhance nighttime warming. High humidity, evaporative cooling, and increased cloud cover suppress shortwave radiation during the day while trapping longwave radiation at night. In contrast, drier southern and inland regions experience reduced evaporative cooling and stronger radiative forcing, leading to larger increases in TXx than TNn<sup>11</sup>.

DTR (Diurnal Temperature Range): DTR quantifies the difference between daily maximum and minimum temperatures, providing insight into differential warming trends. Positive DTR indicates faster warming in maximum temperature than minimum temperature.

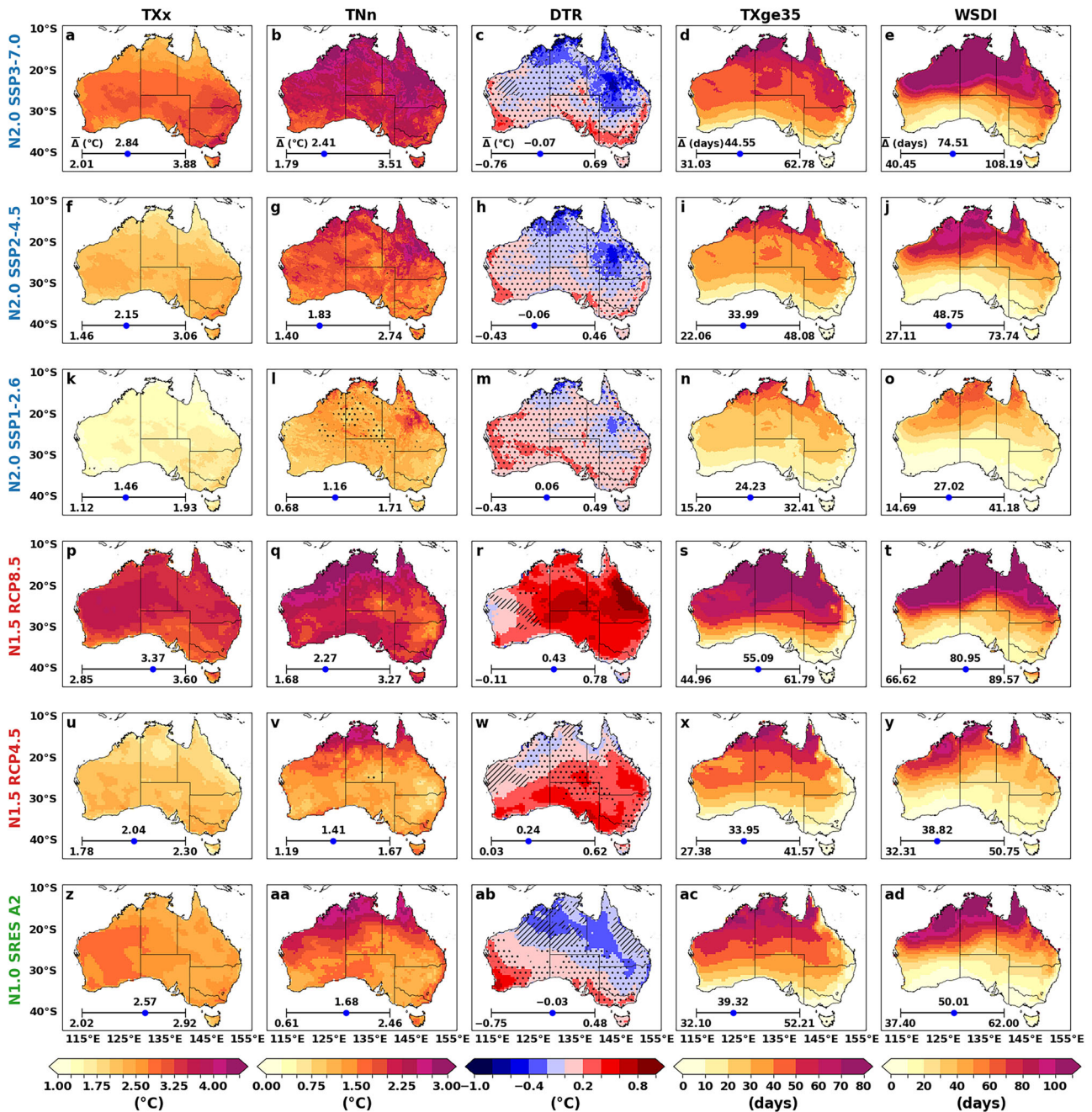


**Fig. 8 | Ensemble mean changes in temperature related extremes for three NARCIIM generations, with significance stippling as per Fig. 2. a–e, f–j, and k–o illustrate changes in temperature extreme indices for NARCIIM2.0 under SSP3-**

**7.0, SSP2-4.5, and SSP1-2.6, respectively. p–t and u–y show the corresponding changes for NARCIIM1.5 under RCP8.5 and RCP4.5, respectively. z–ad present changes in temperature extreme indices for NARCIIM1.0 under SRES A2.**

N2.0 projects a similar DTR change pattern across all three SSPs, with larger magnitudes under higher-emission scenarios (Fig. 8c, h, m, Supplementary Fig. S33). In northern and northeastern Australia, DTR is projected to decrease as minimum temperatures increase more rapidly than maximum temperatures. In contrast, southeastern and southwestern coastal regions show a DTR increase, where maximum temperatures rise faster than minimum temperatures (Figs. 2a, f, k 3a, f, k). Those changes are mostly insignificant.

N1.5 exhibits a markedly different DTR pattern compared to N2.0 under both RCPs. Under RCP8.5, it projects a significant DTR increase across most of Australia, except along the western coast and western Tasmania (Fig. 8r), consistent with a faster rise in maximum than minimum temperatures (Figs. 2p, 3p). Under RCP4.5, significant DTR increases are

concentrated in southern Australia, while the northern regions experience little change or a slight decrease (Fig. 8w). Most of increases in DTR are statistically significant.

N1.0 projects a smaller DTR increase along the southern coast and southwestern Australia but a decrease elsewhere, with the most significant declines in central and northern Australia (Fig. 8ab). This pattern reflects regional differences in temperature trends: maximum temperatures increase more rapidly than minimum temperatures in southwestern Australia but more slowly in northern Australia (Figs. 2z, 3z).

TXge35 (Number of Days with Maximum Temperature  $\geq 35^\circ\text{C}$ ): N2.0 projects a significant increase in TXge35 over northern Australia, with smaller increases over eastern and southern regions, including Tasmania across all three SSPs, with a clear south-to-north gradient. Under the

high-emission scenario (SSP3–7.0), the projected increase falls between those of N1.0 and N1.5 (Fig. 8d, Supplementary Fig. S34), with domain averaged increase of 45 days per year. Under the moderate-emission scenario (SSP2–4.5), the increase (Fig. 8i) is comparable to that projected under RCP4.5 in N1.5 (Fig. 8x), while the low-emission scenario (SSP1–2.6) shows a significantly smaller increase (Fig. 8n). All of increase are statistically significant.

N1.5 shows a spatial pattern of TXge35 increases like N2.0 under both RCPs, but with a much larger domain-averaged increase under RCP8.5—~55 days per year. Under RCP4.5, the projected increase is 34 days per year. N1.0 also projects a similar increase in TXge35 patterns as N1.5 & 2.0, with a domain-averaged increase of approximately 39 days per year.

WSDI (Warm Spell Duration Index): N2.0 projects a significant WSDI increase, particularly over northern Australia, featuring a clear north-to-south decreasing gradient across all three SSPs. Domain averaged WSDI is projected to have more than 75, 49 and 27 additional days for high-, medium- and low emission scenarios. Under the high-emission scenario (SSP3–7.0), the projected increase falls between those of N1.0 and N1.5 (Fig. 8e, Supplementary Fig. S35). For SSP1–2.6, the increase is significantly smaller (Fig. 8o), while projections for SSP2–4.5 (Fig. 8j) lie between the other two scenarios and slightly exceed those under RCP4.5 in N1.5 (Fig. 8y).

N1.5 shows a spatial WSDI increase pattern like N2.0 under both RCPs. Under RCP8.5, it projects a much larger domain-averaged increase of 81 days per year (Fig. 8t). In contrast, under RCP4.5, the projected increase is 39 days, which is much smaller than in N1.0 (Fig. 8y). N1.0 also projects a significant WSDI increase, with a decreasing gradient toward the south (Fig. 8ad). The domain-averaged increase is ~50 days per year.

In summary, all temperature-related extremes—except for DTR—are projected to increase consistently and significantly across all NARCLiM generations, scenarios, and regions. All three NARCLiM generations project rising TXx, TNn, TXge35, and WSDI across scenarios, with larger increases under higher emissions. TXx and TXge35 intensify most in northern Australia, while WSDI shows a north-to-south gradient. TNn increases are smaller than TXx, especially under high-emission scenarios. DTR changes vary, with N2.0 showing mixed patterns and generally insignificant trends, while N1.5 projects significant DTR increases under RCP8.5. These results highlight stronger warming of extreme heat events compared to cold extremes, emphasizing the benefits of emissions mitigation. Projected future changes in temperature extremes for eight state capital cities are summarized in Supplementary Table S6.

Overall, extreme heat indices, except for DTR, are projected to intensify across Australia, with similar spatial patterns across generations but magnitudes increasing with emissions. TXx and TNn are projected rise under global warming, especially in the north, while TXge35 and WSDI show sharp increases in northern Australia, indicating more frequent and severe extreme heat events.

Second, we assess future projections of precipitation-related extremes across the three NARCLiM generations. Five selected precipitation-related indices—CDD, CWD, R10mm, Rx1Day, and R99p—are evaluated and compared below.

CDD (Consecutive Dry Days): N2.0 projects only small changes in CDD across all three SSPs. Under SSP3–7.0, a slight increase is projected across most of the continent, particularly in western Australia, with a domain-averaged rise of 7.57 days (Fig. 9a, Supplementary Fig. S36). For SSP2–4.5, a more scattered decrease is projected, resulting in a domain-averaged change of 3.68 days (Fig. 9f). SSP1–2.6 shows an even more dispersed and modest decrease, with a domain-averaged change of 2.15 days (Fig. 9k).

In contrast, N1.5 projects substantially larger and statistically significant increases in CDD, especially under RCP8.5. The largest increases are seen in central northern Australia, with most of the country showing significant changes (Fig. 9p). The domain-averaged increase reaches 18.26 days per year, with all simulations consistently projecting increases

ranging from 7.1 to 34.64 days. Under RCP4.5, the projected increases are smaller but remain most pronounced in central inland Australia (Fig. 9u).

N1.0, by comparison, shows only small changes in CDD, with a slight inland decrease and small increases elsewhere (Fig. 9z). However, there is considerable variation among individual simulations, ranging from –9 to 14 days, indicating substantial uncertainty in the projections.

CWD (Consecutive Wet Days): N2.0 projects relatively consistent CWD changes across all three SSPs, with noticeable decreases in northern and northeastern Australia, as well as in the southwest and southeast coastal regions, including Tasmania. Small increases are projected inland and in central southern Australia (Fig. 9b, g, l, Supplementary Fig. S37). These patterns align with those projected by all three NARCLiM generations for southern and southwestern coastal areas, including Tasmania.

N1.5 also shows small changes in CWD but with a different spatial pattern from N1.0. Increases over central northern and southeastern Australia, as seen in N1.0, are reduced or reversed to decreases under both RCP8.5 and RCP4.5. Central western Australia, which showed little change in N1.0, exhibits increase in N1.5. Nevertheless, decreases along the southern coasts, Tasmania, and southwestern Australia are consistent across both RCPs.

N1.0 projects relatively minor CWD changes, with decreases in southern Australia (eastern Tasmania, the southwest, and northwest coastal areas) and increases in central northern and southeastern Australia (Fig. 9a). However, these changes are not statistically significant.

R10mm (Days with Precipitation  $\geq$  10 mm): N2.0 projects a consistent pattern of R10mm change across all SSPs, with larger decreases along eastern and western coasts and in Tasmania. Elsewhere, changes are relatively small (Fig. 9c, h, m, Supplementary Fig. S38). These trends align with projected shifts in annual precipitation (Fig. 4a, f, k), indicating that heavy rainfall events are a major driver of total rainfall changes.

N1.5 shows a markedly different R10mm pattern from N1.0, with slight increases in central western Australia, the southeastern coast, and southern Tasmania, but notable decreases elsewhere, particularly in the northern and northeastern coasts (Fig. 9r, w). The magnitude of changes is greater under RCP8.5.

N1.0 projects significant R10mm decreases over southwestern Western Australia, northern Tasmania, and the Great Dividing Range, while increases are seen elsewhere, especially along the central northern coast (Fig. 9ab).

Rx1day (Maximum 1-day Precipitation): N2.0 generally projects result like N1.0 in northern and western Australia under SSP3–7.0 and SSP2–4.5 (Fig. 9d, i, Supplementary Fig. S39) but differs in eastern Australia where small decreases or minimal changes occur. Under SSP1–2.6, slight increases are projected along northern coasts, with inland decreases in northern and eastern Australia (Fig. 9n).

N1.5 shows a different Rx1day pattern, with modest increases in eastern and western Australia, including Tasmania, but decreases in between under RCP8.5, particularly along the northwest coast (Fig. 9s). Under RCP4.5, small coastal increases and inland decreases are projected (Fig. 9x).

N1.0 projects widespread increases in Rx1day, except in small areas of western Australia and northern Queensland. The most significant increases are in northern and southeastern Australia, with a domain-averaged increase of 12.55 mm/day (Fig. 9ac).

R99p (Annual Sum of Daily Precipitation > 99th Percentile): Across all NARCLiM generations and emissions scenarios, changes in R99p closely follow the spatial pattern of Rx1day, though with larger magnitudes (Supplementary Fig. S40). This suggests that changes in R99p are primarily driven by variations in extreme daily precipitation. Projected future changes in precipitation extremes for eight state capital cities are summarized in Supplementary Table S7.

In summary, projections for precipitation extremes vary across NARCLiM generations, though some trends remain consistent. Rx1day, R99p, and CDD are generally projected to increase, while CWD and

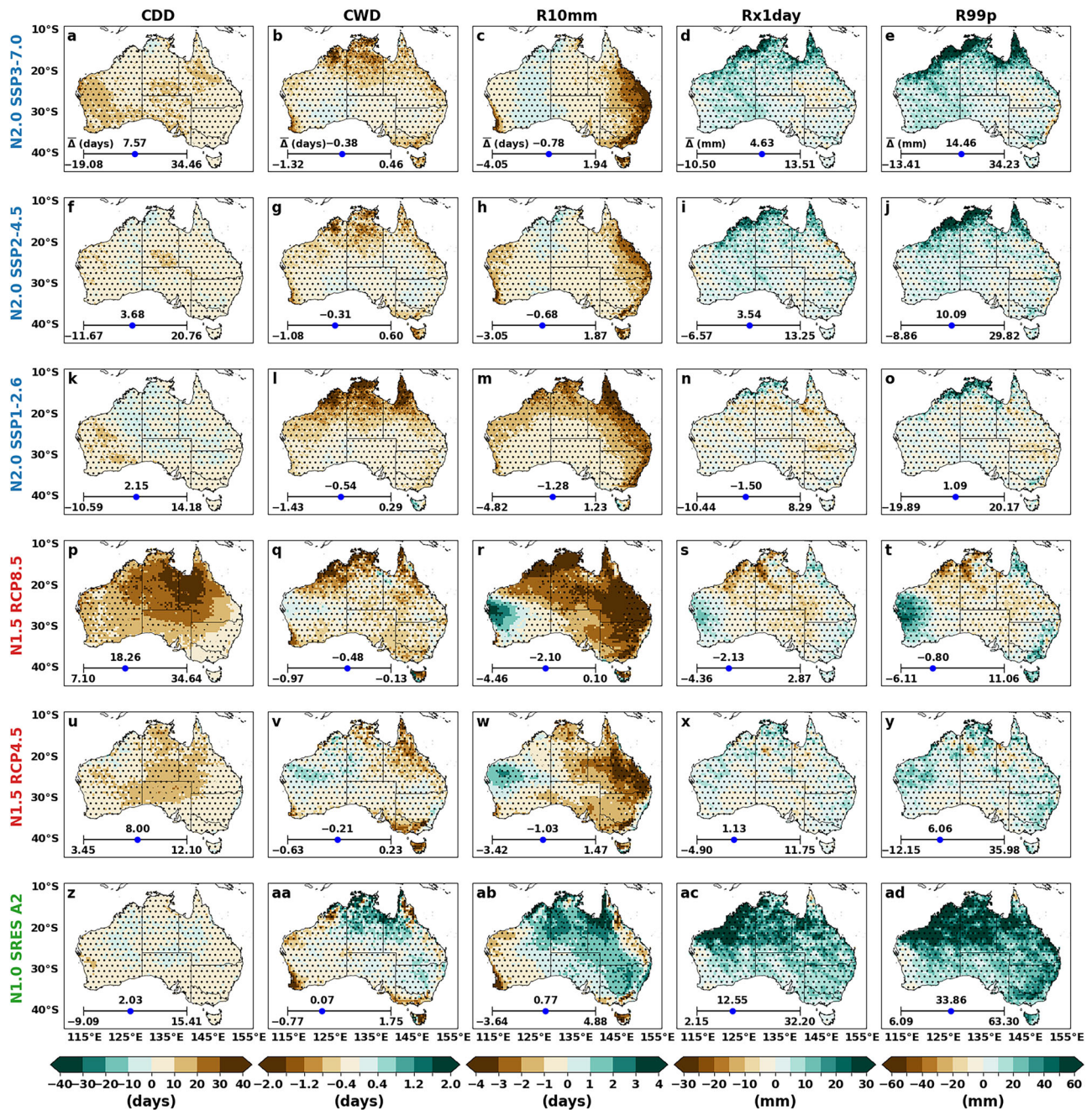


**Fig. 9 | Ensemble mean changes in precipitation related extremes for three NARClM generations, with significance stippling as per Fig. 2. a–e, f–j, and k–o illustrate changes in precipitation extreme indices for NARClM2.0 under SSP3-7.0, SSP2-4.5, and SSP1-2.6, respectively. p–t and u–y show the corresponding changes for NARClM1.5 under RCP8.5 and RCP4.5, respectively. z–ad present changes in precipitation extreme indices for NARClM1.0 under SRES A2.**

R10mm are projected to decrease, with strong regional differences influenced by model generation and emission scenarios, highlighting the complexity of future change in precipitation extremes. N2.0 projections show shorter wet periods and fewer heavy rainfall days, but very extreme precipitation is projected to become more intense.

**Similarities and differences in future projections of climate extremes**

Like the mean climate projections, there are notable similarities across generations. All generations project an increasing trend in TXx, TNn, TXge35, and WSDI, with greater increases under higher emission scenarios. These trends align well with projected future temperature changes in their respective driving GCMs (Fig. 7), indicating that changes in heat extremes

are similarly influenced by these models. Extreme heat increases are consistently largest in northern Australia.

Several consistent trends for precipitation emerge across all generations, including increases in Rx1day, R99p, and CDD, while CWD and R10mm generally show decreases. Higher emissions lead to stronger changes across all indices in each generation, except for CWD and R10mm for N2.0.

However, there are noticeable disagreements between generations. N1.0 projects statistically significant increases in TXx (2.57 °C), particularly over inland regions. N1.5 follows a similar pattern but shows much larger increases (3.37 °C) under RCP8.5. N2.0 lies between N1.0 and N1.5 under high emissions, with lower increases under SSP1–2.6. TNn increases more in northern Australia, with N2.0 showing a stronger warming trend in the

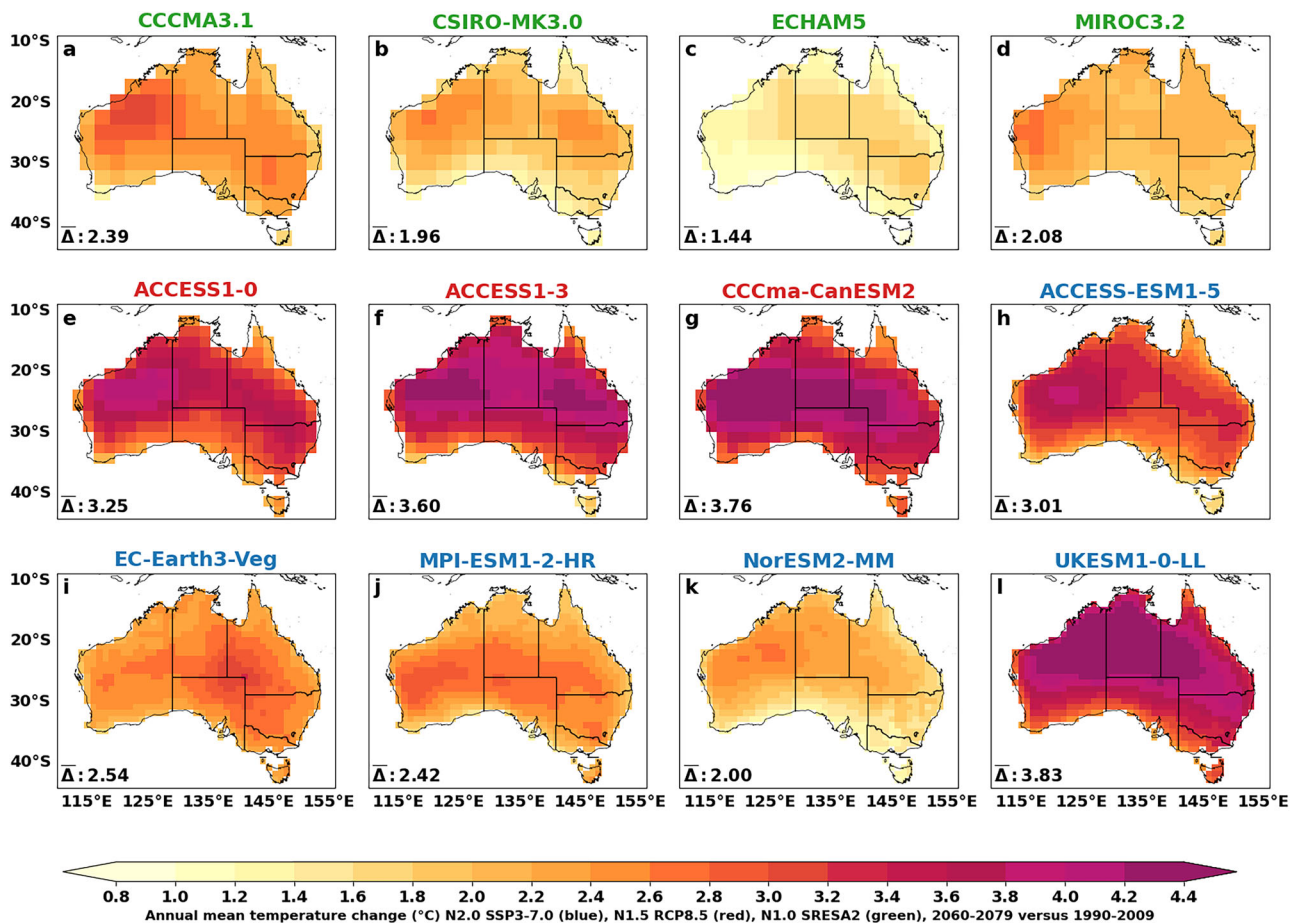


**Fig. 10 | Temperature projection for each GCM used in NARClm for high emission (SSP370, RCP85 and A2) in three NARClm generations. Those with green (a–d), red (e–g) and blue (h–l) titles are the selected CMIP3, CMIP5 and CMIP6 GCMs for N1.0, N1.5 and N2.0 individually.**

northeastern regions. DTR decreases in northern Australia for N1.0 and N2.0 but increases widely in N1.5 under RCP8.5, although these changes are mostly insignificant. TXge35 and WSDI show similar patterns, with N2.0’s projections falling between N1.0 and N1.5, and much smaller increases under lower-emission scenarios.

N1.0 projects minimal changes in CDD, while N1.5 shows significant increases, especially under RCP8.5. N2.0 also projects slight changes (i.e. small increases under SSP3–7.0 and decreases under SSP1–2.6). CWD decreases in southern Australia across all generations, with N1.5 showing more substantial reductions than N1.0. R10mm decreases in southwestern Australia and Tasmania in N1.0 and N2.0, with larger reductions in N1.5. Rx1day generally increases in N1.0, while N1.5 projects decreases in northwest Australia. N2.0 shows similar trends to N1.0 for SSP3–7.0 and SSP2–4.5, but with inland decreases. R99p follows the same trends as Rx1day. It’s worth noting that these changes in precipitation related extremes are mostly statistically insignificant.

In summary, extreme heat intensifies across all generations, while precipitation extremes show regionally varied changes. Overall, heat extremes (TXx, TNn, TXge35, WSDI) intensify across all generations, but N1.5 consistently projects stronger warming under RCP8.5. Projections for precipitation extremes vary significantly across generations and scenarios, with N1.5 showing stronger drying trends, while N2.0 aligns more closely with N1.0. N2.0 also demonstrates clearer mitigation effects under SSP1–2.6, highlighting the role of emissions reductions.

## Discussion

In this study, we compare future climate projections from all of the NARClm generations and investigate plausible causes for the differences in climate change projections across the three generations of NARClm.

So far, we have focused on comparing future projections of the ensemble mean for each NARClm generation, considering both mean and extreme climate variables. Now, we extend our analysis to examine the similarities and differences in future projections between each GCM and its corresponding RCMs within each NARClm generation.

Since some N1.0 GCMs provide only mean temperature instead of maximum and minimum temperature, we assess future changes in mean temperature and precipitation for each GCM across the three NARClm generations. Temperature projections for each GCM used in NARClm are shown in Fig. 10. Generally, GCMs in N1.0 project moderate warming, with mean temperature increases ranging from 1.4 to 2.4 °C. In contrast, the three GCMs in N1.5 project a significantly hotter future, with increases between 3.3 and 3.8 °C. GCMs in N2.0 exhibit a wide range of future temperature changes—some project only slightly warmer conditions than N1.0, while one GCM projects an even hotter future than N1.5. On average, the CMIP5 GCM ensemble projects greater warming than CMIP3 but less than CMIP6 (Fig. 7). The three warmest CMIP5 GCMs were selected for N1.5 to complement N1.0, ensuring representation of a hotter future that was not captured by CMIP3 GCMs (Nishant et al.<sup>16</sup>). In contrast, N2.0 selected GCMs that span the full range of possible future changes in temperature and precipitation<sup>34</sup> (Fig. 7).

In general, the warming projected by GCMs is reflected in their downscaled RCM simulations. For example, UKESM1-0-LL, the hottest of all the GCMs (Fig. 10), drives simulations that project the largest increases in maximum temperature (Supplementary Figs. S16–S20) and heat extremes (TXx, TNn, TXge35, and WSDI) (Supplementary Figs. S31–S32, S34–S35). Similarly, the N1.5 GCMs, which project greater warming than those in other generations, also drive simulations that show much larger increases in maximum temperature and heat extremes. This pattern is consistently

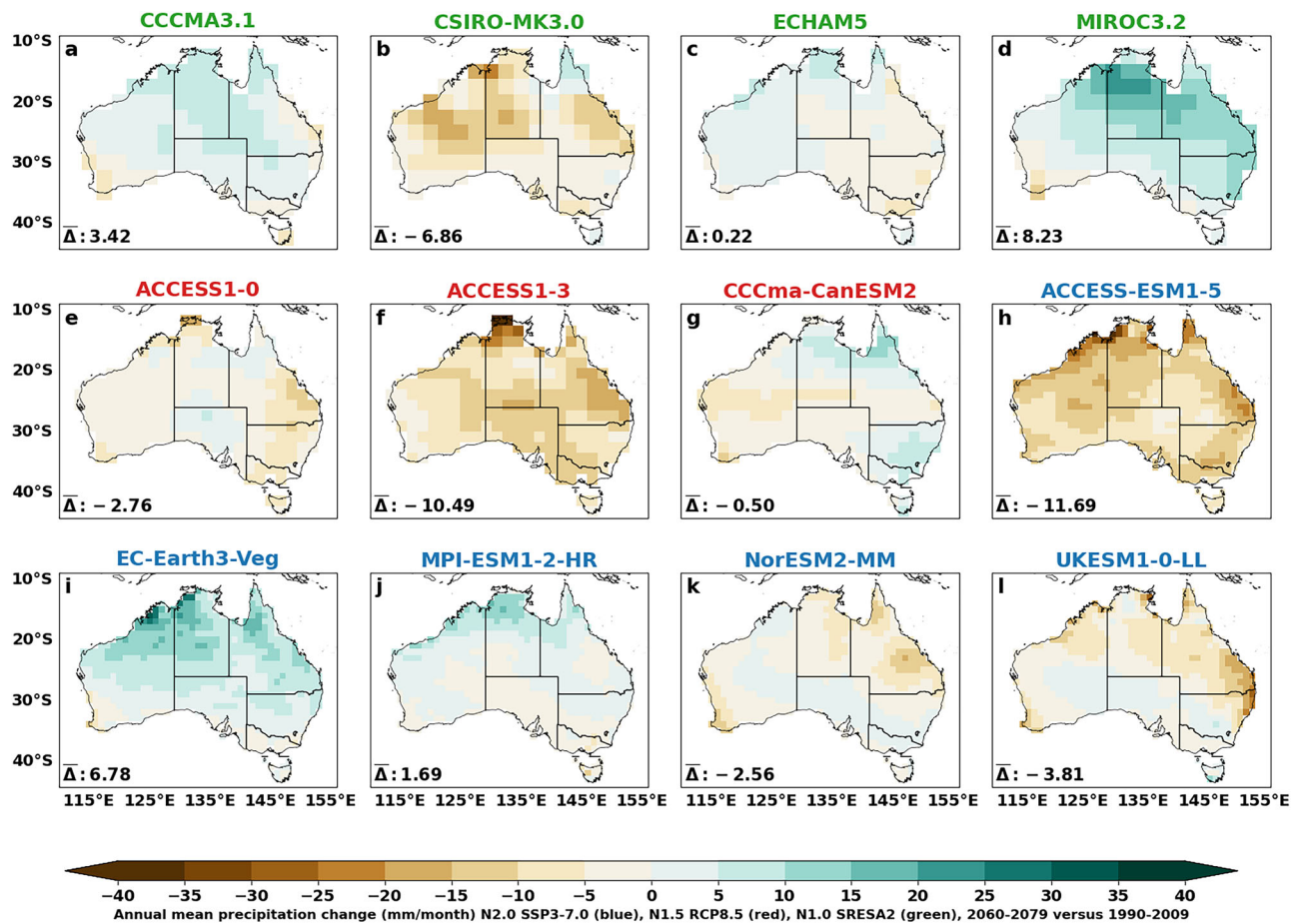


**Fig. 11 | Precipitation projection for each GCM used in NARCLiM for high emission (SSP370, RCP85 and A2) in three NARCLiM generations.** Those with green (a–d), red (e–g) and blue (h–l) titles are the selected CMIP3, CMIP5 and CMIP6 GCMs for N1.0, N1.5 and N2.0 individually.

observed across GCMs within each NARCLiM generation. For instance, the five N2.0 GCMs project different levels of warming (Fig. 10), and their driven RCMs closely follow these patterns in maximum temperature changes (Supplementary Fig. S16).

A similar relationship holds for precipitation. Drier GCMs generally drive drier RCM simulations, and wetter GCMs drive wetter ones. For example, ACCESS-ESM1.5 projects the largest decrease in precipitation (Fig. 11), and its two N2.0-driven RCM simulations exhibit the same trend (Supplementary Figs. S26–30). Within each NARCLiM generation, drier GCMs typically result in drier RCMs. Likewise, wetter GCMs produce wetter RCMs—MIROC3.2 and CCCMA3.1 in N1.0, as well as EC-Earth3-Veg in N2.0, generally project substantial precipitation increases, and their driven RCMs show similar trends. This pattern is evident within each generation: GCMs projecting wetter futures generally lead to wetter RCM simulations.

While GCMs exhibit varying magnitudes of temperature increases and differing signs of precipitation changes (Figs. 10, 11), their downscaled RCM simulations largely follow these projected trends. However, within the same GCM-driven RCM simulations, the magnitude of maximum temperature increase remains consistent (Supplementary Fig. S16), and precipitation change patterns are similar (Supplementary Fig. S26). This indicates that the future projections across the three NARCLiM generations are primarily determined by the selected GCMs.

To enhance the robustness of future RCM projections, a broader selection of GCMs should be considered when downscaling CMIP simulations. This would ensure comprehensive coverage of all possible future changes in temperature and precipitation. However, this is not always possible owing to resource constraints and insufficient availability of requisite sub-daily driving variables from the GCMs.

N2.0 represents a significant advancement over earlier generations (N1.0 and 1.5) through comprehensive updates to model configurations, resolution, and scenario design. In N1.0 and N1.5, GCM selection was based on literature review<sup>15,16</sup>, whereas N2.0 selected five CMIP6 GCMs based on detailed evaluations of both mean climate and climate extremes<sup>34</sup>. Similarly, the regional climate model (RCM) selection process has evolved. While N1.0 and N1.5 relied on 36 WRF physics combinations tested over eight 2-week extreme events, N2.0 implemented a two-stage evaluation: 78 WRF physics combinations were first assessed using 14-month simulations, from which seven high-performing configurations were identified. These were then further evaluated through 41-year simulations to select the final two RCMs for GCM-driven runs. As a result, N2.0 simulations show improved performance compared to earlier versions<sup>17</sup>.

N2.0 employs an updated version of the WRF model (v4.1) with enhanced physical parameterisations and is driven by five carefully selected CMIP6 GCMs, providing a more comprehensive representation of future climate change range. Spatial resolution has been significantly improved—from 50 km to 20 km for the Australasian domain and from 10 km to 4 km for Southeast Australia—enhancing the suitability of projections for local and regional impact assessments. The use of modern emissions scenarios (SSP1–2.6, SSP2–4.5, and SSP3–7.0) ensures alignment with current international climate modelling practices and supports more relevant and timely planning. These enhancements lead to more accurate representation of climate extremes, such as heatwaves and extreme rainfall, which are crucial for risk assessment. In addition, N2.0 features a larger, more robust ensemble that better captures the uncertainty space through diverse GCM–RCM pairings. The project is further strengthened by strong stakeholder engagement and inter-jurisdictional collaboration, ensuring that its

documentation, support tools, and datasets are accessible and tailored to the needs of researchers, planners, and policymakers.

In each NARCLiM generation, we aimed to select the best-performing and most independent GCMs and RCMs for downscaling. However, decision to select GCMs was constrained by data limitations and availability.

In N1.0, three of the top-performing and most preferred GCMs could not be used because they lacked the required sub-daily data<sup>15,35</sup>. As a result, some GCMs included in N1.0 were not the most ideal choices for accurately simulating the Australian climate, affecting the overall performance of the ensemble. Similarly, N1.5 was designed to include a wet GCM, a GCM with little change in precipitation, and a dry GCM to ensure a diverse range of climate scenarios. However, data availability constraints led to the exclusion of the wet GCM, preventing full representation of the intended range of precipitation outcomes.

Compared to N1.0 and N1.5, the selection process for N2.0 involved a more comprehensive evaluation of GCMs and RCMs to ensure the ideal set of available models was used<sup>34</sup>. Despite this thorough assessment, some of the preferred GCMs remained unusable due to the absence of necessary sub-daily data<sup>14</sup>.

To address these recurring challenges, we suggest that the WCRP (World Climate Research Programme) Working Group on Coupled Modelling (WGCM) establish guidelines for modelling groups to provide the essential sub-daily (at least six-hourly) three-dimensional variables in future CMIPs. Ensuring the availability of these data would significantly enhance dynamical downscaling efforts and improve GCM selection for regional climate modelling projects like NARCLiM.

These challenges highlight the critical importance of data availability and standardization in climate modelling. By ensuring that future climate models include the necessary high-resolution data, the accuracy and reliability of regional climate projections can be greatly improved.

In this study, our focus was on comparing similarities and differences in the projections of mean and extreme climate across three generations of NARCLiM. We also sought to understand the sources of variation in these projections, with the goal of identifying the strengths and weaknesses of each generation. However, we did not aim to diagnose the underlying cause of model differences between simulations within each generation and across generations. In Australia, precipitation is influenced by multiple weather systems, and their representation in simulations is particularly important for regional precipitation projections. Pepler and Dowdy<sup>36</sup> reported a projected decrease in the frequency of deep midlatitude cyclones under a warming climate, although their intensity is expected to increase. Dey et al.<sup>37</sup> reviewed historical and projected changes in Australian rainfall and emphasized the importance of key weather systems and climate drivers in shaping future rainfall patterns. Future work applying the recently released Multi-Object Analysis of Atmospheric Phenomena (MOAAP; Prein et al.<sup>38</sup>) is planned to evaluate the NARCLiM simulations for their ability to capture these key systems and to assess links between future changes in weather systems and projected precipitation. These analyses will help us understand the underlying process to result in projected changes in mean climate and climate extremes.

In this study, we also applied statistical significance tests to mean climate and extreme indices and followed the approach of Tebaldi et al.<sup>39</sup> to assess model agreement in ensemble-mean future projections. However, we did not explicitly evaluate field significance. Instead, our analysis emphasized spatially consistent patterns across ensemble members and generations, which helps reduce the likelihood that results are driven by random noise. Future work will incorporate field significance testing using a Monte Carlo framework.

Building on the findings of the NARCLiM project, future research could focus on several key areas:

Convection-permitting models (CPMs) represent an important advancement in regional climate modelling, as they explicitly resolve convective processes that are only parameterized in coarser-resolution models. This enables a more realistic simulation of rainfall intensity, duration, and spatial distribution, as well as improved representation of temperature and

other fine-scale climate features<sup>40</sup>. In N2.0, the use of 4 km CPMs provides an opportunity to better capture local-scale climate processes and extreme events, such as heavy rainfall, heatwaves, and convective storms, which are often poorly represented in models with 10 km or coarser resolution. Assessing the performance of these CPMs against observations is crucial to evaluate their added value over previous NARCLiM generations. Furthermore, using these high-resolution models to project future climate conditions will help improve our understanding of potential changes in climate extremes and their impacts across southeastern Australia.

Where driving data permit, incorporating a broader range of GCMs into regional climate studies can better capture the range of plausible future climates and enhance the robustness of impact assessments. Given the high computational cost of dynamical downscaling, it is not feasible to downscale all GCMs. However, four modelling groups in Australia have used different GCMs to drive different regional climate models (RCMs)<sup>11,12</sup>.

Recent work by Jiang et al.<sup>13</sup> compared simulations driven by GCMs across multiple RCMs. Their results suggest that GCM-driven simulations show consistent performance across different RCMs. Key ensemble-wide model biases include dry biases in northern and southern Australia, wet winter biases, and a persistent underestimation of winter diurnal temperature range across all modelling centres. Daily variability at large spatial scales appears comparable between GCMs and RCMs, while long-term trends are largely governed by the driving GCM.

These findings highlight the value of assessing projections generated by the same GCM driving multiple RCMs. Preliminary analysis, for instance, shows that four RCMs driven by ACCESS-ESM1-5 project broadly similar changes in temperature and precipitation. Further analysis is needed to quantify similarities and differences in such configurations. If strong agreement is observed among simulations using the same GCM, then simulations using different GCMs from the four modelling groups could be integrated into a “super ensemble” to improve the reliability of future projections and reduce uncertainties.

Even the best-performing GCMs have biases that are passed to the RCM via the boundary conditions. Recent work has demonstrated that bias correction of the GCM data before use results in improved RCM simulations<sup>41–45</sup>, although this could potentially limit the spread of the RCM simulations.

Recent advances in statistical and deep learning downscaling have shown promise for translating GCM outputs to local scales<sup>46–50</sup> although some statistical downscaling approaches focus on the mean and therefore have a sort of built-in bias correction. While these methods typically focus on a limited set of climate variables—unlike dynamical downscaling that offers a full suite—they are computationally efficient and can be applied across a large number of GCMs. Evaluating and comparing the performance of these approaches could inform their integration into future projection frameworks, potentially expanding the diversity of downscaled products available.

As highlighted in Ji et al.<sup>17</sup>, more systematic efforts are needed to identify and prioritise the best-performing RCMs. Selecting models with lower historical biases can substantially reduce the uncertainty in future climate projections.

While NARCLiM projections are typically based on multi-model ensembles to provide an overall picture of future climate, individual ensemble members could be strategically used for specific applications. For instance, drier ensemble members could inform worst-case drought planning, whereas wetter projections may be useful for flood risk assessment. This targeted use can enhance the relevance and applicability of climate projections for sector-specific planning.

By advancing research in these areas, future work can build on the success of the NARCLiM project, further improving regional climate modelling and contributing to stronger climate resilience and sustainability efforts.

In this study, we examine the similarities and differences in future climate projections across three generations of NARCLiM, focussing on both mean and extreme climate changes. The objective is to understand the sources of variation in projections among these generations.

Temperature projection patterns are broadly consistent across all NARCLiM generations, with the magnitude of change largely reflecting the trends of their driving GCMs. Emission scenarios also play a critical role—lower emissions pathways generally result in less severe temperature increases. These increases are statistically significant across simulations, underscoring the robustness of warming projections.

In contrast, precipitation projections show substantial variability across generations, primarily driven by differences in the GCMs used for downscaling. This highlights the inherent complexity of simulating precipitation changes and the strong dependence on GCM selection.

Extreme heat is projected to intensify across all generations, while changes in precipitation extremes vary by region. Heat-related extremes (e.g., TXx, TNn, TXge35, WSDI) increase significantly in all simulations, with N1.5 consistently projecting stronger warming under RCP8.5. Notably, TXx increases more rapidly than annual maximum temperature, whereas TNn increases more slowly than annual minimum temperature.

Precipitation extremes show greater divergence. N1.5 projects stronger drying trends, while N2.0 aligns more closely with N1.0. Importantly, N2.0 demonstrates clearer mitigation signals under SSP1–2.6, emphasizing the impact of emissions reduction on future precipitation extremes. These changes in both heat and precipitation extremes are largely governed by the choice of driving GCMs, nevertheless with notable spatial variability in the downscaled simulations. Overall, future climate projections across the three NARCLiM generations are primarily determined by the driving GCMs, as the RCMs tend to preserve the large-scale trends projected by the GCMs.

A key limitation of NARCLiM lies in the availability of suitable data from the driving GCMs. Several desirable models could not be included due to the lack of required sub-daily (at least 6-hourly), three-dimensional variables. This underscores the need for a coordinated global effort to ensure future CMIP datasets provide the necessary data for dynamical downscaling.

To improve the robustness of future RCM-based projections, a broader ensemble of GCMs should be incorporated into downscaling efforts. This would help ensure a more comprehensive representation of plausible future changes in temperature and precipitation. Given computational constraints, alternative approaches such as statistical and deep learning-based downscaling may also offer promising additional avenues for regional future projections.

The findings of this study are critical to inform the design of future downscaling projects, highlighting the importance of diverse GCM selection to enhance the reliability and comprehensiveness of regional climate projections.

## Methods

### Climatology and major weather systems of Australia

To assist interpretation of our results, we first provide an overview of Australia’s climatology and the key processes that shape it. Climate in Australia exhibits strong spatial and seasonal variability<sup>51</sup>. Maximum temperatures peak in the northern and central interior, often exceeding 40 °C in summer, with extremes above 45 °C. The tropical north remains hot year-round (>35 °C), while southern and coastal regions are milder (25–35 °C in summer, 10–20 °C in winter). The Australian Alps are much cooler (14–22 °C in summer and 0–6 °C in winter). Minimum temperatures range from >20 °C in the north to below 5 °C in southern Australia and Tasmania during winter. Rainfall is also highly variable: the north is dominated by the summer monsoon, the east receives year-round rainfall, the arid interior is dry, and southern and western regions are wetter in winter.

Precipitation in Australia is controlled by multiple weather systems. In the north, tropical cyclones, the summer monsoon, and convective thunderstorms dominate<sup>37,52,53</sup>, with cyclones contributing ~30% of annual rainfall and >40% of extremes<sup>54</sup>. The monsoon is strongly modulated by ENSO (El Niño Southern Oscillation), MJO (Madden-Julian Oscillation), and IOD (Indian Ocean Dipole), and has increased in intensity in northwest Australia since 1920<sup>52</sup>. Remnant cyclones and storms also influence central regions. In the south, precipitation arises mainly from fronts, east coast lows, and blocking highs<sup>55</sup>. Declining frontal rainfall reflects weaker westerlies and more anticyclones<sup>56</sup>, while thunderstorm rainfall has increased<sup>57</sup>. Collectively, these systems account for ~86% of rain days and >98% of rainfall for southern Australia (south of 25°S). Consequently, changes in their frequency, duration, or intensity have profound implications for Australia’s precipitation patterns.

### Three generations of NARCLiM and ET-SCI extremes

This section provides a brief description of three NARCLiM generations. Their major features are summarized in Table 1; see Di Virgilio et al.<sup>14</sup> for further details.

The first generation of NARCLiM, referred to as N1.0, was developed to produce high-resolution climate projections for the Australasian region, with a particular focus on Southeast Australia<sup>15,58</sup>. To achieve this, a nested modelling domain was established, employing a one-way nesting approach: a 10-km resolution inner domain over Southeast Australia was embedded within a 50-km resolution outer domain, aligned with the CORDEX Australasia region (see Fig. 1).

The primary objective of N1.0 was to dynamically downscale CMIP3 GCMs using a regional climate modelling framework. Four GCMs were selected based on a literature review assessing their performance in simulating Australia’s recent climate, the independence of their biases, their coverage of the full range of projected futures for Southeast Australia, and

**Table 1 | Major features of the three generations of NARCLiM**

	Model generation		
	NARCLiM1.0	NARCLiM1.5	NARCLiM2.0
Release date	2014	2020	2024
Years simulated	1990–2009, 2020–2039, 2060–2079	1950–2100	1950–2100
Grid resolutions: CORDEX-Australasia; NARCLiM inner domains	50 km; 10 km	50 km; 10 km	20 km; 4 km
Vertical levels	30	30	45
Global climate models	4 CMIP3 GCMs CCCMA3.1, ECHAM5, MIROC3.2, CSIRO-mk3.0	3 CMIP5 GCMs ACCESS1.0, ACCESS1.3, CanESM2	5 CMIP6 GCMs ACCESS-ESM1-5, EC-Earth3-Veg, MPI-ESM1-2-HR, NorESM2-MM, UKESM1-0-LL
Regional climate models	3 RCM configurations (WRF3.3)	2 RCM configurations (WRF3.6.0.5)	2 RCM configurations (WRF4.1.2)
Future emission scenarios	SRES A2	RCP4.5, RCP8.5	SSP1–2.6, SSP2–4.5, SSP3–7.0
Reanalysis-driven (CORDEX evaluation)	NCEP: 1950–2009	ERA-Interim: 1979–2013	ERA5: 1979–2020

the availability of data for downscaling. Collectively, these four GCMs represented the range of projected changes in temperature and precipitation within the CMIP3 ensemble.

The Weather Research and Forecasting (WRF) model version 3.3<sup>59</sup> was employed as the Regional Climate Model (RCM). Three combinations of WRF physics parameterizations were selected from an initial set of 36 combinations of WRF physics, chosen based on model performance and the independence of their errors<sup>15,60–62</sup>.

The selected four GCMs and three RCMs were combined to produce 12 GCM/RCM simulations. Each simulation covered three 20-year time slices: the recent past (1990–2009), the near future (2020–2039), and the far future (2060–2079), under the SRES A2 emissions scenario<sup>63</sup>. Additionally, each RCM configuration was driven by the NCEP reanalysis dataset<sup>64</sup> for the period 1950–2009 to establish a historical baseline. N1.0 required ~10 million CPU hours and generated over 350 TB of data.

Building on the successes and insights from N1.0, the second phase, N1.5, was developed to dynamically downscale CMIP5 GCMs, thereby expanding the range of projected future climates. N1.5 was specifically designed to complement N1.0 by capturing climate futures that were not adequately sampled by the original CMIP3-based ensemble.

A comparative assessment within the climate futures framework revealed that CMIP5 included a subset of models projecting warmer and drier futures, which were absent from the CMIP3 GCMs used in N1.0<sup>16</sup>. To address this gap, three CMIP5 GCMs were selected using the same methodology applied in N1.0—evaluating performance in simulating the historical Australian climate, independence of biases, and coverage of ensemble spread<sup>15</sup>.

Each selected GCM was dynamically downscaled using two of the original three RCM configurations from N1.0—specifically, R1 and R2—over the same nested modelling domains. The R3 configuration was excluded due to its relatively poor performance in simulating maximum temperature when driven by ERA-Interim reanalysis data over 1981–2010<sup>25</sup>.

Simulations were run continuously from 1950 to 2100, using an updated version of the WRF model (v3.6, compared to v3.3 used in N1.0). Each GCM-RCM pairing was forced under two future emissions scenarios, RCP4.5 and RCP8.5, providing a broader sampling of plausible climate futures to support impact and adaptation research.

N1.5 has a smaller ensemble size than N1.0; however, its simulations cover the continuous period from 1951 to 2100, rather than three discrete 20-year periods as in N1.0 and include two emission scenarios. This experiment required approximately 20 million CPU hours and produced over 800 TB of output data.

The third and most advanced phase of the NARCLiM project, N2.0, marks a major advancement in regional climate modelling through the use of convection-permitting simulations. The inner domain resolution over Southeast Australia was increased from 10 km (in N1.0 and N1.5) to 4 km, allowing explicit representation of convective processes<sup>65,66</sup>. This eliminates the need for cumulus parameterization at 4 km, improving the simulation of extreme weather events and local-scale processes. The outer domain resolution was increased from 50 km to 20 km, and the number of vertical levels increased from 30 to 45, with more levels added in lower troposphere. However, the model top remains the same as N1.0 and N1.5.

N2.0 downscales CMIP6 GCMs, selected based on performance, bias independence, diversity of projected changes, and data availability<sup>14,34</sup>. A rigorous evaluation of 78 WRF configurations resulted in two high-performing RCMs chosen for GCM driven simulations<sup>67,68</sup>.

Five GCMs were used, with projections run under three SSP (Shared Socioeconomic Pathway) scenarios: SSP1–2.6, SSP2–4.5, and SSP3–7.0 (Van Vuuren et al.<sup>31</sup>). Notably, N2.0 adopted SSP3–7.0 as the high-emission pathway, following CORDEX recommendations ([https://cordex.org/wp-content/uploads/2021/02/CORDEX-CMIP6\\_exp\\_design\\_draft\\_SOD\\_In.pdf](https://cordex.org/wp-content/uploads/2021/02/CORDEX-CMIP6_exp_design_draft_SOD_In.pdf)), distinguishing it from N1.5's RCP8.5 (Supplementary Tables S1, 2), with lower radiative forcing (7.0 W/m<sup>2</sup> vs. 8.5 W/m<sup>2</sup>).

N2.0 employed higher spatial resolution, a larger ensemble, and additional emission scenarios, resulting in substantially greater computational demands than earlier generations. These simulations required over 300 million CPU hours and produced more than 16.7 PB of data.

Ji et al.<sup>17</sup> evaluated and compared the performance of three generations of NARCLiM in simulating observed mean maximum and minimum temperatures, precipitation, and ten selected climate extremes. Their findings show that N2.0 offers substantial improvements in simulating mean maximum temperature and precipitation, along with related extremes such as TXx, TXge35, CDD, and R99p. It significantly reduces biases in the mean climate, particularly over southeast Australia, and notably lowers domain-averaged absolute biases for all extremes except TNn, compared to earlier versions. These improvements in N2.0 are largely attributable to advances in RCM design—including enhanced model physics and higher resolution—and result in lower domain-averaged absolute biases and thus increase the value of the simulations for climate impact assessments, providing greater confidence in future projections. Overall, these improvements suggest that N2.0 provides a more reliable basis for climate impact assessments and future planning.

The transition from N1.0 to N2.0 highlights the continuous evolution in regional climate modelling capabilities, driven by advancements in GCMs, RCMs, and downscaling methodologies. Each generation builds on the strengths and addresses the limitations of its predecessors, delivering increasingly accurate and valuable climate projections for the Australasian region.

### The expert team on sector-specific climate indices (ET-SCI)

Extreme climate and weather events are inherently complex. In this study, we assess climate extremes based on daily precipitation and temperature, following the definitions established by the Expert Team on Sector-specific Climate Indices (ET-SCI)<sup>69,70</sup>. The N1.0 and N1.5 ET-SCI indices were generated using ClimPACT version 2 (<https://climpact-sci.org/>), incorporating daily precipitation as well as maximum and minimum temperatures.

The N2.0 ET-SCI indices were derived using iclim version 6.5.0<sup>71</sup> and xclim version 0.49.0<sup>72</sup>. Iclim and xclim adhere to the European Climate Assessment & Dataset (ECA&D; [https://etccdi.pacificclimate.org/list\\_27\\_indices.shtml](https://etccdi.pacificclimate.org/list_27_indices.shtml)) definition, whereas ClimPACT follows the Expert Team on Climate Change Detection and Indices (ETCCDI; <https://www.ecad.eu/indicesextremes/indicesdictionary.php>) definition.

Test comparisons between ET-SCI indices generated using ClimPact, iclim and xclim showed no substantial differences in these outputs. However, ClimPact uses R, whereas the entire index postprocessing software workflow developed for N2.0 uses Python, hence, xclim and iclim were used for N2.0 ET-SCI production because they offer xarray multi-processing in Python.

We selected 10 extreme climate indices (Table 2) based on the following criteria: 1) Capturing key aspects of climate extremes – these include absolute indices (e.g., maximum 1-day precipitation [Rx1day], hottest day [TXx], coldest day [TNn]), threshold-based indices (e.g., number of heavy rain days [R10mm], number of days with maximum temperature equal to or exceeding 35 °C [TXge35]), percentile-based indices (e.g., total annual precipitation from very heavy rain days [R99p]), and duration indices (e.g., consecutive wet days [CWD], consecutive dry days [CDD], warm spell duration index [WSDI]). 2) Assessing extremes with significant societal and infrastructural impacts – for example, TXge35 and WSDI are strongly linked to public health risks<sup>73</sup>, while R99p, Rx1day, diurnal temperature range (DTR), CDD, and CWD have substantial implications for agriculture, water resources, and economic stability<sup>74,75</sup>.

### Method of future projection

Future climate projections for mean precipitation, maximum and minimum temperatures, along with 10 selected climate extremes are calculated as the changes between future and historical periods. We assess these changes both annually and seasonally, considering the absolute changes in

**Table 2 | Selected ET-SCI extremes**

No	Index	Definition	Units	Timescale	Sectors
1	TXx	Warmest daily maximum temperature	°C	Annual/Monthly	Agriculture and food security, energy, forestry/GHGs, cryosphere
2	TNn	Colest daily minimum temperature	°C	Annual/Monthly	Agriculture and food security, energy, forestry/GHGs, cryosphere
3	DTR	Diurnal temperature range	°C	Annual/Monthly	Forestry/GHGs
4	TXge35	Count of number of days when maximum temperature $\geq 35$ °C	days	Annual/Monthly	Health, agriculture and food security, disaster risk reduction, energy, forestry/GHGs
5	WSDI	Warm spell duration indicator (Annual number of days contributing to events where 6 or more consecutive days experience maximum temperature > 90th percentile)	days	Annual	Health, agriculture and food security, water resources and food security, coasts, disaster risk reduction, energy, fisheries, forestry/GHGs, cryosphere
6	CDD	Consecutive dry days (Maximum number of consecutive dry days (when precipitation < 1.0 mm))	days	Annual	Health, agriculture and food security, water resources and food security, disaster risk reduction, forestry/GHGs
7	CWD	Consecutive wet days (Maximum annual number of consecutive wet days (when precipitation $\geq 1.0$ mm))	days	Annual	Coasts
8	Rf10mm	Count of number of days when precipitation is at least 10mm	days	Annual/Monthly	Coasts
9	Rx1Day	Maximum 1-day precipitation	mm	Annual/Monthly	Agriculture and food security, water, coasts, disaster risk reduction, forestry/GHGs
10	R99p	Total annual precipitation from very heavy precipitation days (Annual sum of daily precipitation > 99th percentile)	mm	Annual	Coasts

each variable. As N1.0 only has three non-consecutive period with each of 20-year, we select the historical period of 1990–2009 and one future projection period of 2060–2079 for fair comparisons among these three generations of NARCLiM.

In our analysis, we aim to provide a detailed understanding of how climate variables are expected to change in the future. This includes examining the magnitude of changes in temperature, precipitation and their extremes, as well as the spatial variability of these changes across Australia. We also extracted future projections of mean and extreme climate for eight state capital cities (Fig. 1). By comparing the projections from different model generations, we can identify trends and patterns that are consistent across models, enhancing the robustness of our projections. It also provides valuable information for decision-makers and users from a climate services perspective.

The statistical significance of annual and seasonal future projections was assessed for each grid cell. For maximum and minimum temperatures, *t* tests ( $\alpha = 0.05$ ) assuming equal variance were used. Due to the non-normality of precipitation data, the Mann–Whitney U test was applied.

Following Tebaldi et al.<sup>39</sup>, the statistical significance of each ensemble mean was categorized as follows: 1) Statistically Insignificant Areas (Stippled): Fewer than 50% of RCMs exhibit significant changes. 2) Areas of Significant Agreement (Coloured): At least 50% of RCMs show significant changes, with at least 66% of them agreeing on the change sign. This indicates a consistent change across models. 3) Areas of Significant Disagreement (Hatched): At least 50% of RCMs show significant changes, but fewer than 66% agree on the change sign. This categorization helps assess the reliability of model outputs, highlighting regions with consistent changes and improving the interpretation of climate projections for climate change adaptation planning.

### Data availability

Data for NARCLiM 2.0 is made available via National Computing Infrastructure (NCI) under <https://doi.org/10.25914/ysxb-rt43> or through NCI THREDDS Data Server <https://thredds.nci.org.au/thredds/catalog/catalogs/zz63/catalog.html>. NARCLiM1.0 and 1.5 are made available via the New South Wales Climate Data Portal (<https://climatedata-beta.environment.nsw.gov.au/>).

### Code availability

The Weather Research and Forecasting (WRF) version 4.1.2 used in NARCLiM2.0 is freely available from: <https://github.com/coecms/WRF/tree/V4.1.2>. The underlying code for this study is not publicly available but may be made available to qualified researchers on reasonable requests from the corresponding author.

Received: 3 September 2025; Accepted: 21 November 2025;

Published online: 14 January 2026

### References

- Ekström, M., Grose, M. R. & Whetton, P. H. An appraisal of downscaling methods used in climate change research. *Wiley Interdiscip. Rev. Clim. Change* **6**, 301–319 (2015).
- Jacob, D. et al. EURO-CORDEX: new high-resolution climate change projections for European impact research. *Reg. Environ. Change* **14**, 563–578 (2014).
- Kjellström, E. et al. Production and use of regional climate model projections—a Swedish perspective on building climate services. *Clim. Serv.* **2**, 15–29 (2016).
- Skelton, M., Porter, J. J., Dessai, S., Bresch, D. N. & Knutti, R. The social and scientific values that shape national climate scenarios: a comparison of the Netherlands, Switzerland and the UK. *Reg. Environ. Change* **17**, 2325–2338 (2017).
- Christensen, J., Carter, T., Rummukainen, M. & Amanatidis, G. Evaluating the performance and utility of regional climate models: the PRUDENCE project. *Clim. Change* **81**, 1–6 (2007).

6. van der Linden, P. & Mitchell, J. F. B. (eds) *ENSEMBLES: Climate Change and its Impacts. Summary of Research and Results from the ENSEMBLES Project* (Met Office Hadley Centre, 2009).
7. Fu, C. et al. Regional climate model intercomparison project for Asia. *Bull. Am. Meteorol. Soc.* **86**, 257–266 (2005).
8. Mearns, L. O. et al. The North American Regional Climate Change Assessment Program: overview of phase I results. *Bull. Am. Meteorol. Soc.* **93**, 1337–1362 (2012).
9. Solman, S. A. et al. Evaluation of an ensemble of regional climate model simulations over South America driven by the ERA-Interim reanalysis: model performance and uncertainties. *Clim. Dyn.* **41**, 1139–1157 (2013).
10. Giorgi, F. & Jones, C. Addressing climate information needs at the regional level: the CORDEX framework. *WMO Bull.* **58**, 175–183 (2009).
11. Chapman, S. et al. Evaluation of dynamically downscaled CMIP6-CCAM models over Australia. *Earths Future* **11**, e2023EF003548 (2023).
12. Howard, E. et al. Performance and process-based evaluation of the BARPA-R Australasian regional climate model version 1. *Geosci. Model Dev.* **17**, 731–757 (2024).
13. Jiang, X. et al. Towards benchmarking the dynamically downscaled CMIP6 CORDEX-Australasia ensemble over Australia. *J. South. Hemis. Earth Syst. Sci.* **75**, ES24050 (2025).
14. Di Virgilio, G. et al. Design, evaluation and future projections of the NARCLiM2.0 CORDEX-CMIP6 Australasia regional climate ensemble. *Geosci. Model Dev.* **18**, 671–702 (2025).
15. Evans, J. P. et al. Design of a regional climate modelling projection ensemble experiment: NARCLiM. *Geosci. Model Dev.* **7**, 621–629 (2014).
16. Nishant, N. et al. Introducing NARCLiM1.5: evaluating the performance of regional climate projections for southeast Australia for 1950–2100. *Earths Future* **9**, e2020EF001833 (2021).
17. Ji, F. et al. Three generations of NARCLiM: evaluation of precipitation, temperature and their extremes over the CORDEX Australasia domain. *Int. J. Climatol.* [https://papers.ssrn.com/sol3/papers.cfm?abstract\\_id=5391058](https://papers.ssrn.com/sol3/papers.cfm?abstract_id=5391058) (2025).
18. Olson, R., Evans, J. P., Di Luca, A. & Argüeso, D. The NARCLiM project: model agreement and significance of climate projections. *Clim. Res.* **69**, 209–227 (2016).
19. Evans, J. P., Argüeso, D. & Olson, R. Bias-corrected regional climate projections of extreme rainfall in southeast Australia. *Theor. Appl. Climatol.* **130**, 1085–1098 (2017).
20. Herold, N. et al. Projected changes in the frequency of climate extremes over southeast Australia. *Environ. Res. Commun.* **3**, 011001 (2021).
21. Evans, J. P., Kay, M., Prasad, A. & Pitman, A. The resilience of Australian wind energy to climate change. *Environ. Res. Lett.* **13**, 024014 (2018).
22. Di Luca, A., Evans, J. P. & Ji, F. Australian snowpack in the NARCLiM ensemble: evaluation, bias correction and future projections. *Clim. Dyn.* **50**, 3946–3960 (2018).
23. Ji, F. et al. Projected change in characteristics of near-surface temperature inversions for southeast Australia. *Clim. Dyn.* **52**, 1487–1503 (2019).
24. Ji, F. et al. Projected changes in vertical temperature profiles for Australasia. *Clim. Dyn.* **55**, 3921–3940 (2020).
25. Di Virgilio, G. et al. Evaluating reanalysis-driven CORDEX regional climate models over Australia: model performance and errors. *Clim. Dyn.* **53**, 2985–3005 (2019a).
26. Di Virgilio, G. et al. Climate change increases the potential for extreme wildfires. *Geophys. Res. Lett.* **46**, 8517–8526 (2019b).
27. Ji, F. et al. Introducing NARCLiM1.5: evaluation and projection of climate extremes for southeast Australia. *Weather Clim. Extremes* **37**, 100526 (2022).
28. Ji, F. et al. Rapid warming in the Australian Alps from observations and NARCLiM simulations. *Atmosphere* **13**, 1686 (2022).
29. Evans, J. P. et al. The CORDEX-Australasia ensemble: evaluation and future projections. *Clim. Dyn.* **56**, 1207–1226 (2021).
30. Wilson, L. et al. A national hydrological projections service for Australia. *Clim. Serv.* **18**, 100331 (2022).
31. Van Vuuren, D. P. et al. The representative concentration pathways: an overview. *Clim. Change* **109**, 5–31 (2011).
32. Collins, M. et al. Long-term climate change: Projections, commitments and irreversibility. In *Climate Change 2013: The Physical Science Basis. Contribution of Working Group I to the Fifth Assessment Report of the Intergovernmental Panel on Climate Change* 1029–1136 (Cambridge Univ. Press, 2013).
33. Riahi, K. et al. The Shared Socioeconomic Pathways and their energy, land use, and greenhouse gas emissions implications: an overview. *Glob. Environ. Change* **42**, 153–168 (2017).
34. Di Virgilio, G. et al. Selecting CMIP6 GCMs for CORDEX dynamical downscaling: Model performance, independence, and climate change signals. *Earths Future* **10**, e2021EF002625 (2022).
35. Evans, J. P. & Ji, F. *Choosing GCMs*. NARCLiM Tech. Note 1, 7 (NARCLiM Consortium, 2012).
36. Pepler, A. & Dowdy, A. Fewer deep cyclones projected for the midlatitudes in a warming climate, but with more intense rainfall. *Environ. Res. Lett.* **16**, 054044 (2021).
37. Dey, R., Lewis, S. C., Arblaster, J. M. & Abram, N. J. A review of past and projected changes in Australia's rainfall. *WIREs Clim. Change* **10**, e577 (2019).
38. Prein, A. F., Mooney, P. A. & Done, J. M. The multi-scale interactions of atmospheric phenomena in mean and extreme precipitation. *Earths Future* **11**, e2023EF003534 (2023).
39. Tebaldi, C., Arblaster, J. M. & Knutti, R. Mapping model agreement on future climate projections. *Geophys. Res. Lett.* **38**, L23701 (2011).
40. Zou, L. W. & Zhou, T. J. Convection-permitting simulations of current and future climates over the Tibetan Plateau. *Adv. Atmos. Sci.* **41**, 1901–1916 (2024).
41. Kim, Y., Rocheta, E., Evans, J. P. & Sharma, A. Impact of bias correction of regional climate model boundary conditions on the simulation of precipitation extremes. *Clim. Dyn.* **55**, 3507–3526 (2020).
42. Kim, Y., Evans, J. P. & Sharma, A. Multivariate bias correction of regional climate model boundary conditions. *Clim. Dyn.* **61**, 3253–3269 (2023a).
43. Kim, Y., Evans, J. P. & Sharma, A. Correcting biases in regional climate model boundary variables for improved simulation of high-impact compound events. *iScience* **26**, 107696 (2023b).
44. Kim, Y., Evans, J. P. & Sharma, A. A software for correcting systematic biases in RCM input boundary conditions. *Environ. Model. Softw.* **168**, 105799 (2023c).
45. Kim, Y., Evans, J. P. & Sharma, A. Correcting multivariate biases in regional climate model boundaries: How are synoptic systems impacted over the Australian region? *Geophys. Res. Lett.* **51**, e2024GL111445 (2024).
46. Nishant, N. et al. Comparison of a novel machine learning approach with dynamical downscaling for Australian precipitation. *Environ. Res. Lett.* **18**, 095012 (2023).
47. Liu, D. L. & Zuo, H. P. Statistical downscaling of daily climate variables for climate change impact assessment over New South Wales, Australia. *Clim. Change* **115**, 629–666 (2012).
48. Cuan, P. et al. Estimating the impact of projected climate change on runoff across the tropical savannas and semiarid rangelands of northern Australia. *J. Hydrometeorol.* **13**, 483–503 (2012).
49. Teng, J. et al. Assessment of an analogue downscaling method for modelling climate change impacts on runoff. *J. Hydrol.* **472**, 111–125 (2013).
50. Fu, G. B. et al. Modelling runoff with statistically downscaled daily site, gridded and catchment rainfall series. *J. Hydrol.* **492**, 254–265 (2013).

51. Liu, D. L. et al. Characterising rainfall changes in 1960–2019 for continental Australia. *Int. J. Climatol.* **40**, 6855 (2020).
52. Heidemann, H. et al. Variability and long-term change in Australian monsoon rainfall: a review. *WIREs Clim. Change* **14**, e823 (2023).
53. Heidemann, H., Narsey, S. & Brown, J. What drives interannual rainfall variability over northern Australia? *J. Geophys. Res. Atmos.* **130**, e2024JD043016 (2025).
54. Lavender, S. L. & Abbs, D. J. Trends in Australian rainfall: contribution of tropical cyclones and closed lows. *Clim. Dyn.* **40**, 317–326 (2013).
55. Pepler, A. Projections of synoptic anticyclones for the twenty-first century. *Clim. Dyn.* **61**, 3271–3287 (2023).
56. Pepler, A. S. & Rudeva, I. Anomalous subtropical zonal winds drive decreases in southern Australian frontal rain. *Weather Clim. Dyn.* **4**, 175–188 (2023).
57. Pepler, A. S., Dowdy, A. J. & Hope, P. The differing role of weather systems in southern Australian rainfall between 1979–1996 and 1997–2015. *Clim. Dyn.* **56**, 2289–2302 (2021).
58. Evans, J. P. & Ji, F. *Choosing the RCMs to Perform the Pownscaling*. NARCIIM Tech. Note 2, 8 (NARCIIM Consortium, Sydney, Australia, 2012).
59. Skamarock, W. C. et al. *A Description of the Advanced Research WRF Version 3*. NCAR Tech. Note (NCAR, 2008).
60. Evans, J. P., Ekström, M. & Ji, F. Evaluating the performance of a WRF physics ensemble over south-east Australia. *Clim. Dyn.* **39**, 1241–1258 (2012).
61. Evans, J. P., Ji, F., Abramowitz, G. & Ekström, M. Optimally choosing small ensemble members to produce robust climate simulations. *Environ. Res. Lett.* **8**, 044050 (2013).
62. Ji, F., Ekström, M., Evans, J. P. & Teng, J. Evaluating rainfall patterns using physics scheme ensembles from a regional atmospheric model. *Theor. Appl. Climatol.* **115**, 297–304 (2014).
63. Solomon, S., Manning, M., Marquis, M. & Qin, D. *Climate Change 2007 – The Physical Science Basis: Working Group I Contribution to the Fourth Assessment Report of the IPCC* (Cambridge Univ. Press, 2007).
64. Kalnay, E. et al. The NCEP/NCAR 40-year reanalysis project. *Bull. Am. Meteorol. Soc.* **77**, 437–472 (1996).
65. Kendon, E. J., Prein, A. F., Senior, C. A. & Stirling, A. Challenges and outlook for convection-permitting climate modelling. *Philos. Trans. R. Soc. A* **379**, 20190547 (2021).
66. Lucas-Picher, P. et al. Convection-permitting modelling with regional climate models: Latest developments and next steps. *WIREs Clim. Change* **12**, e731 (2021).
67. Di Virgilio, G. et al. Evaluation of CORDEX ERA5-forced ‘NARCIIM2.0’ regional climate models over Australia using the Weather Research and Forecasting (WRF) model version 4.1.2. *Geosci. Model Dev.* **18**, 703–724 (2025).
68. Ji, F. et al. Evaluation of precipitation extremes in ERA5-driven regional climate simulations over the CORDEX-Australasia domain. *Weather Clim. Extremes* **44**, 100676 (2024).
69. Alexander, L. V. & Herold, N. Climpactv2 indices and software. Commission for Climatology Expert Team on Sector-Specific Climate Indices (ET-SCI), [https://epic.awi.de/id/eprint/49274/1/ClimPACTv2\\_manual.pdf](https://epic.awi.de/id/eprint/49274/1/ClimPACTv2_manual.pdf) (2015).
70. Herold, N. & Alexander, L. Climpact2 software. <https://github.com/ARCCSS-extremes/climpact2> (2016).
71. Pagé, C. & Aoun, A. *iclim: Calculating Climate Indices and Indicators Made Easy* (Authorea, 2022).
72. Bourgault, P. et al. xclim: xarray-based climate data analytics. *J. Open Source Softw.* **8**, 5415 (2023).
73. Zivin, J. G. & Shrader, J. Temperature extremes, health, and human capital. *Future Child* **26**, 31–50 (2016).
74. Tabari, H. Climate change impact on flood and extreme precipitation increases with water availability. *Sci. Rep.* **10**, 1–10 (2020).
75. Pei, F., Zhou, Y. & Xia, Y. Assessing the impacts of extreme precipitation change on vegetation activity. *Agriculture* **11**, 487 (2021).

## Acknowledgements

This research was supported by the New South Wales Department of Climate Change, Energy, the Environment and Water as part of the NARCIIM2.0 dynamical downscaling project contributing to CORDEX Australasia. Funding was provided by the NSW Climate Change Adaptation Strategy and NSW Climate Change Fund for NSW and Australian Regional Climate Modelling (NARCIIM) Project. This research was undertaken with the assistance of resources and services from the National Computational Infrastructure (NCI), which is supported by the Australian Government. J.P.E. acknowledges the support of the Australian Research Council Centre of Excellence for 21st Century Weather (CE230100012) and the Climate Systems Hub of the Australian Governments National Environmental Science Program.

## Author contributions

Fei Ji : Conceptualization, Methodology, Validation, Formal analysis, Investigation, Writing – original draft. Moutassem El Rafei : Methodology, Software, Formal analysis, Investigation, Visualization, Writing – Review & Editing. Giovanni Di Virgilio : Project Administration, Conceptualization, Methodology, Investigation, Visualization, Supervision, Writing –Review & Editing. Jason P. Evans, Jatin Kala, Julia Andrys : Formal analysis, Investigation, Validation, Writing –Review & Editing. Eugene Tam, Stephen White : Data Curation, Validation, Writing –Review & Editing. Dipayan Choudhury, Rishav Goyal, Carlos Vieira Rocha, Yue Li : Validation, Writing –Review & Editing. Matthew L. Riley : Resources, Supervision, Funding Acquisition, Writing –Review & Editing.

## Competing interests

The authors declare no competing interests.

## Additional information

**Supplementary information** The online version contains supplementary material available at <https://doi.org/10.1038/s41612-025-01280-w>.

**Correspondence** and requests for materials should be addressed to Fei Ji.

**Reprints and permissions information** is available at <http://www.nature.com/reprints>

**Publisher’s note** Springer Nature remains neutral with regard to jurisdictional claims in published maps and institutional affiliations.

**Open Access** This article is licensed under a Creative Commons Attribution-NonCommercial-NoDerivatives 4.0 International License, which permits any non-commercial use, sharing, distribution and reproduction in any medium or format, as long as you give appropriate credit to the original author(s) and the source, provide a link to the Creative Commons licence, and indicate if you modified the licensed material. You do not have permission under this licence to share adapted material derived from this article or parts of it. The images or other third party material in this article are included in the article’s Creative Commons licence, unless indicated otherwise in a credit line to the material. If material is not included in the article’s Creative Commons licence and your intended use is not permitted by statutory regulation or exceeds the permitted use, you will need to obtain permission directly from the copyright holder. To view a copy of this licence, visit <http://creativecommons.org/licenses/by-nc-nd/4.0/>.

© The Author(s) 2026